

12

AD-A232 973

David Taylor Research Center

Bethesda, MD 20084-5000

DTRC-SME-90/92 October 1990

Ship Materials Engineering Department
Research and Development Report



A Framework for 3-D Nonlinear Modeling of Thick-Section Composites

by
David A. Pecknold

DTRC-SME-90/92 A Framework for 3-D Nonlinear Modeling of Thick-Section Composites

DTIC
ELECTE
MAR 03 1991
S E D



Approved for public release; distribution is unlimited.

91 3 07 084

MAJOR DTRC TECHNICAL COMPONENTS

- CODE 011 DIRECTOR OF TECHNOLOGY, PLANS AND ASSESSMENT
 - 12 SHIP SYSTEMS INTEGRATION DEPARTMENT
 - 14 SHIP ELECTROMAGNETIC SIGNATURES DEPARTMENT
 - 15 SHIP HYDROMECHANICS DEPARTMENT
 - 16 AVIATION DEPARTMENT
 - 17 SHIP STRUCTURES AND PROTECTION DEPARTMENT
 - 18 COMPUTATION, MATHEMATICS & LOGISTICS DEPARTMENT
 - 19 SHIP ACOUSTICS DEPARTMENT
 - 27 PROPULSION AND AUXILIARY SYSTEMS DEPARTMENT
 - 28 SHIP MATERIALS ENGINEERING DEPARTMENT

DTRC ISSUES THREE TYPES OF REPORTS:

1. **DTRC reports, a formal series**, contain information of permanent technical value. They carry a consecutive numerical identification regardless of their classification or the originating department.
2. **Departmental reports, a semiformal series**, contain information of a preliminary, temporary, or proprietary nature or of limited interest or significance. They carry a departmental alphanumeric identification.
3. **Technical memoranda, an informal series**, contain technical documentation of limited use and interest. They are primarily working papers intended for internal use. They carry an identifying number which indicates their type and the numerical code of the originating department. Any distribution outside DTRC must be approved by the head of the originating department on a case-by-case basis.

David Taylor Research Center

Bethesda, MD 20084-5000

DTRC-SME-90/92 October 1990

Ship Materials Engineering Department
Research and Development Report

A Framework for 3-D Nonlinear Modeling of Thick-Section Composites

by
David A. Pecknold

Accession For	
NTIS GRA&I	<input checked="" type="checkbox"/>
DTIC TAB	<input type="checkbox"/>
Unannounced	<input type="checkbox"/>
Justification	
By	
Distribution/	
Availability Codes	
Dist	Avail and/or Special
A-1	



CONTENTS

	Page
LIST OF TABLES	iv
LIST OF FIGURES	v
ACKNOWLEDGMENTS	1
ABSTRACT	1
ADMINISTRATIVE INFORMATION	1
1 INTRODUCTION	2
2 THICK-SECTION LAMINATES	2
2.1 Compression Test Methods	3
2.2 Conditions at Interfaces between Laminae	3
3 ROLE OF MATERIAL MODELS IN NONLINEAR STRUCTURAL ANALYSIS	4
3.1 Solution of Nonlinear Structural Systems	4
3.2 Material Point Computations	5
4 MATERIAL MODEL	6
4.1 Micro Model	6
4.2 Sublaminar Model	12
5 EVALUATION OF MODEL ARCHITECTURE	18
5.1 Lamina Micro Model	18
5.2 Sublaminar Model	19
6 NONLINEARITIES	22
7 SUMMARY AND CONCLUSIONS	26
8 DEVELOPMENT PLAN	27
9 REFERENCES	28

LIST OF TABLES

Table 1	Graphite and Epoxy Properties used in Comparisons with FE Micromechanical Modeling	30
Table 2	Fiber and Matrix Properties used for Prediction of Lamina Properties	30
Table 3	Lamina Properties for AS4/3501-6 Prepreg Tape	31
Table 4	Lamina Properties for S2 glass/3501-6 Prepreg Tape	32
Table 5	Smearred Properties for 96-ply Laminates	33

LIST OF FIGURES

Figure 1	Interface Conditions Between Adjacent Laminae	34
Figure 2	Material Points (Gauss Integration Points) for Tracking Material Response	35
Figure 3	Numerical Solution of Nonlinear Structural Equations; Illustrating Internal Force I and Residual R	36
Figure 4	Incremental-Iterative Solutions of Nonlinear Structural Equilibrium Equations	36
Figure 5	Material Modeling for Thick-Section Modeling	37
Figure 6	Micro Model for Lamina	38
Figure 7	Sublaminar Model	39
Figure 8	Schematic (one-dimensional) View of Stress Update Illustrating the Difference between σ_{n+1} and $\sigma_n + d\sigma_{n+1}$	40
Figure 9	Lamina Micro-Model vs FE Micromechanical Modeling	41
Figure 10	Lamina Micro-Model - Material Element A Only	42
Figure 11	Thick-Walled Model Cylinder	43
Figure 12	Compression Response of $[0_2/90]_{16s}$	44
Figure 13	Bending Response of $[0_2/90]_{16s}$	46
Figure 14	Compression Response of $[0_2/90]_s$	48
Figure 15	Bending Response of $[0_2/90]_s$	50

ACKNOWLEDGEMENTS

The author is grateful for the support of Mr. J.J. Kelly, the Program Area Manager for Materials of the DARPA ASTP program.

ABSTRACT

An architecture is proposed for three-dimensional nonlinear material modeling of thick-section composite laminates which may have thicknesses ranging from 1/4 in. up to several inches. In this thickness range, there is very little applications-related experience or experimental information available; the potential effects of out-of-plane stresses and strains on material properties and behavior are therefore of great concern.

The material model is intended to be used as a component of a standard finite element structural analysis package; this places several practical limits on material model complexity. The model consists of two main components: a lamina micro-model containing fiber and matrix elements and a simplified unit-cell analysis; and a sublaminar model based on a 3D lamination theory which enforces equilibrium of out-of-plane stresses.

A wide variety of nonlinear material behavior descriptions can be incorporated in the fiber and matrix constitutive models; a nonlinear elastic power-law model which reflects matrix shear-softening response is formulated. Approaches for modeling kink-banding and interply delamination are discussed. Excellent agreement is shown with detailed elastic finite element micromodeling of a graphite/epoxy laminate, with DTRC thick-section compression tests of graphite/epoxy and glass/epoxy laminates, and with exact ply-by-ply elasticity solutions for a thick cylinder.

ADMINISTRATIVE INFORMATION

This project was supported by the DTRC Independent Research program, sponsored by the Office of Chief of Naval Research, Director of Naval Research, OCNR 10, and administered by Dr. Bruce Douglas (Code 0112) under Program Element 61152, Task Area R000N00 and DTRC Work Unit 2844-220.

1. Introduction

This report describes a framework for the development of 3-D nonlinear material models for the structural analysis of thick-section laminated composite structures.

The proposed class of models are predictive; that is, they are based on simplified micro-mechanical analysis and allow predictions of material and structural behavior to be made, proceeding from known or assumed properties of fiber and matrix constituents.

The material model is designed to function through a standard interface with structural analysis packages; the micro-model and sublaminar model which together constitute the two-level material model are hidden from element and structural-level processes.

Essential features of the modeling approach are emphasized; within this basic architecture, various options are available for modeling specific types of nonlinearity, including delaminations. A nonlinear elastic model for matrix behavior is proposed for initial implementation.

The material model architecture is evaluated in the linear elastic range by separately exercising its two components: the micro-model gives excellent agreement with published results of detailed elastic finite element micromodeling of a graphite/epoxy laminate, and with compression loaded $[90]_{96}$ laminates tested at DTRC; the sublaminar model likewise shows excellent agreement with DTRC compression tests of $[0_2/90]_{16}$ laminates and with exact ply-by-ply elasticity solutions for a thick cylinder.

Purely phenomenological approaches may also be viable; however, these typically require voluminous amounts of experimental data. Predictive capabilities are still needed in order to quickly and cheaply evaluate new material systems.

2. Thick-Section Laminates

As a working definition, a *thick-section* laminate may be considered to be one with thickness $t \geq 1/4$ in. Relatively little experimental data is available in this thickness range, particularly for compressive loads (Camponeschi 1989b).

For these thick laminates, it is natural to seek a fully three-dimensional characterization of mechanical properties and behavior, even though it is not yet known precisely when such comprehensive information may be essential for analysis/design.

The term "thick-section" carries no implication regarding the expected character of stress distributions in the composite structure or component. Therefore, it does not follow that a 3-D thick-section material model must necessarily be used in a full-blown 3-D *stress analysis*; only that accurate material constitutive information is available for determining out-of-plane stresses and strains, and for evaluating associated failure criteria.

2.1. Typical Thick-Section Laminate Construction

Thick-section graphite/epoxy or glass/epoxy composite laminates may have thicknesses ranging from 1/4 in. up to several inches. The laminate is often constructed from unidirectional plies each approximately .005 in. thick; it may therefore consist of literally hundreds of individual plies, arranged in a regular stacking sequence.

Thus ply-by-ply analysis, often used in analysis of thin-sections, is not feasible. However, the very large number of plies typical of thick-section laminates produces a structure which is, in effect, much more homogeneous than one with a small number of plies; this feature of thick-section laminates allows a homogenization or "smearing" procedure to be used effectively at the laminate level.

2.2. Conditions at Interfaces between Laminae

Fig. 1 shows a typical lamina subjected to a three dimensional state of average or nominal stress. These stresses represent effective values averaged over typical unit cells at the microscopic level. The reinforcing fibers lie in the $x-y$ plane in Fig. 1; the z axis is the thickness direction. The stresses are grouped into *in-plane* ($\sigma_x, \sigma_y, \tau_{xy}$), and *out-of-plane* stresses ($\sigma_z, \tau_{yz}, \tau_{xz}$). Strains are grouped in the same way into in-plane strains ($\epsilon_x, \epsilon_y, \gamma_{xy}$), and out-of-plane strains ($\epsilon_z, \gamma_{yz}, \gamma_{xz}$).

The conditions at the interface are:

1. On the top and bottom surfaces of the lamina, where it is assumed to be perfectly bonded to adjacent laminae, *displacement continuity* requires that the *in-plane strains* ($\epsilon_x, \epsilon_y, \gamma_{xy}$) be continuous across interfaces.

2. *Equilibrium* requires that *out-of-plane stresses* ($\sigma_z, \tau_{yz}, \tau_{xz}$) be continuous across interfaces.

Where elastic properties change across interfaces, the complementary quantities (out-of-plane strains and in-plane stresses) can be discontinuous.

Classical Laminate Theory (CLT) for thin-sections ignores the second interface condition, on the assumption that the out-of-plane stresses are negligible, and that the in-plane stresses and strains can be accurately determined without considering interface equilibrium.

The apparent difficulty of satisfying equilibrium of out-of-plane stresses, within the framework of conventional modeling and structural analysis methods, has concerned many researchers (Christensen 1988) and has led to attempts to develop so-called hybrid and mixed finite element methods for analysis of thick laminated shells.

The approach proposed here addresses these concerns without resorting to unconventional methods.

3. Role of Material Model in Nonlinear Structural Analysis

Structural modeling usually employs numerically-integrated parametric finite elements. This element family, which includes line, surface and solid elements, provides a flexible geometric modeling capability and a systematic approach for all element level computations.

Fig. 2 shows a schematic view of a finite element model. A typical 20-node isoparametric element is shown, with a set of *material points*, or Gaussian integration points (2x2x3 integration).

These material points are the basic building blocks of the structural model. They are the locations at which stresses, strains and loading history variables are tracked. Each discrete material point is taken to represent the behavior of some finite volume of material in the neighborhood of that point; if the idealization is too coarse, more material points are used. Ply-by-ply monitoring of material response and behavior, in the context of thick-sections, would correspond to the use of hundreds of material points through the thickness of the laminate, which is clearly not required.

The material model operates at these material points and performs two important tasks: (1) stress updates; and (2) tangent stiffness updates, if required.

3.1. Solution of Nonlinear Structural Systems

The solution of nonlinear systems is usually carried out via a combined incremental-iterative procedure. Modified Newton-Raphson (MNR) is the most widely-used method.

The loads are applied in increments P_n, P_{n+1}, \dots ; at any load step, equilibrium is only approximately satisfied in the numerical solution, as shown in Fig. 3, i.e.

$$I_n = P_n - R_n \quad (1)$$

in which I_n is the internal force vector and R_n is the residual load at step n .

An incremental-iterative solution scheme

$$K_t \Delta U_{n+1}^{(i)} = P_{n+1} - I_{n+1}^{(i-1)} \quad (2)$$

for the nonlinear equilibrium equations is illustrated in Fig. 4. K_t is the tangent stiffness, the displacement increment $\Delta U_{n+1} \equiv U_{n+1} - U_n$, and the superscripts in Eq. (2) are iteration indices.

Referring to Eq. (2), at each iteration: (1) the internal force vector must be updated, and (2) the tangent stiffness may be updated, depending on solution strategy. Both of these operations require computation from the material model.

3.2. Material Point Computations

The current internal force \mathbf{I}_e for the structure is calculated by assembling element contributions \mathbf{I}_e , which in turn are numerically integrated from material point contributions by

$$\mathbf{I}_e = \sum_{MP_i} W_i J_i \mathbf{B}_i^T \boldsymbol{\sigma}_i \quad (3)$$

in which $\boldsymbol{\sigma}_i$ are the stresses at the material point i . Most of the computation involved in Eq. (3) is contained in the evaluation of the updated stress $\boldsymbol{\sigma}_i$ at each material point.

The tangent stiffness \mathbf{K}_e is calculated by assembling element contributions \mathbf{K}_e , which are numerically integrated from material point contributions by

$$\mathbf{K}_e = \sum_{MP_i} W_i J_i \mathbf{B}_i^T \mathbf{C}_i \mathbf{B}_i \quad (4)$$

in which \mathbf{C}_i is the material tangent stiffness, relating incremental stresses to incremental strains at material point i .

Strain increments, previous total stress and strain, and history parameters are passed to the material model, which then updates history parameters, stresses, and material tangent stiffness at the material point. Geometric nonlinearities, if present, appear in the strain-displacement matrix \mathbf{B}_i .

The stress-update and other algorithms in the material model are invoked a very large number of times in any realistic nonlinear analysis. This must be kept clearly in mind when developing nonlinear material models which are intended for use in structural analysis and design.

Consider as an example, a structural analysis involving a thick laminated cylindrical shell modeled with 24-node parametric elements (3 nodes through thickness by 8 nodes in plane): a realistic mesh might be, say, 24 elements circumferentially (15 degree intervals) by 15 elements in the longitudinal direction. Such a mesh has about 10,000 degrees-of-freedom, which is moderately large for nonlinear problems at the present time (1990). To estimate the number of times that the material model would be called, assume a (2x2x3) integration rule and 10 load steps with an average of 4 iterations per step. The material model would be called about 200,000 times (10 inc x 4 iter/inc x 360 el x 12 mp/el = 172,800). If each material model call used 1 CPU-second, the material model computations alone would require about 50 CPU-hours.

This estimate brings into focus the essential importance of fast, efficient algorithms for material model computations.

4. Material Model

The material model consists of two main components illustrated in Fig. 5:

- (1) a *micro-model*, which describes the response of a unidirectional lamina, starting from fiber and matrix constitutive descriptions, and,
- (2) a *sublaminar model*, which generates the response of a typical repeating sublaminae which is constructed from several uni-directional laminae.

The essential structure of these two models will first be developed; specific descriptions of material nonlinearities will be discussed later.

4.1. Micro-Model

The micro-model, if it is to form part of a structural analysis package, must be reasonably simple.

Detailed micro-mechanical modeling, using finite element modeling of typical repeating unit cells, (Adams 1974, Chen and Cheng 1970) is much too computationally-intensive for this purpose. In addition, these models necessarily incorporate a particular unit cell geometry.

Simpler displacement-based micro-models, with several tens of degrees-of-freedom (Pindera et al 1990, Aboudi 1990) have also been proposed. These are essentially crude finite-element models, which use simplified unit cell geometries with rectangular fiber cross-sections. These models are quite accurate compared to more detailed finite element micro-mechanical models, but are still too complicated for a structural analysis package.

At the other end of the spectrum, various smearing procedures, including "rule-of-mixtures" are available (Hashin and Rosen 1964, Hermans 1967, Whitney 1967, Behrens 1971).

Clearly, the complexities in unit cell analysis result from local geometry effects and the accompanying non-uniform stress and strain conditions in the unit cell. The approach used here is intermediate between the latter two categories of micro-models described above. It is essentially a smearing approach, in which average stresses and a simplified unit cell geometry with square fiber cross-sections (Fig. 6) are used.

Stress and Strain Smearing in Unit Cell

The stress and strain smearing procedure is illustrated by the analogs shown in the lower part of Fig. 6. They are intended to schematically represent the load paths in the unit cell.

The unit-cell-average stresses and strains are labelled with the subscripts (1,2,3). The 1-axis is the fiber direction, the 2-axis lies in the plane of the lamina, and the 3-axis is the thickness direction.

There are 3 distinct material elements in the unit cell model, represented by the 3 spring elements in the analog models in Fig. 6; one of these is a fiber element, and the remaining two are matrix elements.

The load path through these material elements is different for axial effects than for transverse effects; for axial (11-direction) stress and strain, the material elements function "in parallel", that is, the 11-direction strains are the same in all three elements as indicated by the schematic in the lower left portion of Fig. 6. This leads to the "rule-of-mixtures" for axial stresses - which is known to be accurate for this case.

The assumed load path for the remaining components (22,12,33,23,13) can be visualized by considering the unit-cell-average transverse stress σ_{33} and the corresponding strain ϵ_{33} . If σ_{33} is applied to the upper and lower horizontal boundaries of the unit cell shown in Fig. 6, there are two parallel stress paths available; one through a matrix element (height 1 and width $1 - \sqrt{V}$) and the second through the series-connected fiber (\sqrt{V} by \sqrt{V}) and matrix ($1 - \sqrt{V}$ by \sqrt{V}) elements. This is illustrated by the analog in the lower right portion of Fig. 6. In the series-connected fiber and matrix elements, the stresses are the equal, and the strains are combined by rule-of-mixtures.

The smearing procedure for the unit-cell is now set down more formally.

First, for convenience, group the three material elements into two sub-groups: *Material Element A*, consisting of the fiber element and the series-or-parallel connected matrix element, and *Material Element B*, consisting of the remaining matrix element.

Material Elements A and B are connected in parallel for all component directions, that is, their strains are the same, and the unit-cell-average stresses are weighted averages of the stresses in A and B. That is,

$$\begin{aligned} [\epsilon]_C &= [\epsilon]_A = [\epsilon]_B \\ [\sigma]_C &= w_f [\sigma]_A + w_m [\sigma]_B \end{aligned} \quad (5)$$

in which the stresses and strains are (6x1) vectors, the subscript C stands for the unit-cell-averages, and w_f and w_m are weighting factors, defined as

$$w_f = \sqrt{V} \quad w_m = 1 - \sqrt{V} \quad (6)$$

Within Material Element A, the axial (11) components are treated differently from the remaining components, as explained above. In order to express the equilibrium and compatibility conditions compactly, the stress and strain vectors are partitioned as follows:

Thus σ_a and ϵ_a are (1x1), and σ_b and ϵ_b are (5x1). The relationships for Material Element A are

$$\begin{bmatrix} \sigma \end{bmatrix} = \begin{bmatrix} \sigma_{11} \\ \sigma_{22} \\ \tau_{12} \\ \sigma_{33} \\ \tau_{23} \\ \tau_{13} \end{bmatrix} \equiv \begin{bmatrix} \sigma_a \\ \sigma_b \end{bmatrix} \quad \begin{bmatrix} \epsilon \end{bmatrix} = \begin{bmatrix} \epsilon_{11} \\ \epsilon_{22} \\ \gamma_{12} \\ \epsilon_{33} \\ \gamma_{23} \\ \gamma_{13} \end{bmatrix} \equiv \begin{bmatrix} \epsilon_a \\ \epsilon_b \end{bmatrix} \quad (7)$$

$$\begin{bmatrix} \epsilon_a \\ \sigma_b \end{bmatrix}_A = \begin{bmatrix} \epsilon_a \\ \sigma_b \end{bmatrix}_f = \begin{bmatrix} \epsilon_a \\ \sigma_b \end{bmatrix}_m \quad (8)$$

$$\begin{bmatrix} \sigma_a \\ \epsilon_b \end{bmatrix}_A = W_f \begin{bmatrix} \sigma_a \\ \epsilon_b \end{bmatrix}_f + W_m \begin{bmatrix} \sigma_a \\ \epsilon_b \end{bmatrix}_m$$

in which the subscripts f and m denote fiber and matrix elements in Material Element A, respectively. The weighting factors W_f and W_m are given by Eq. (6). Note that the vectors shown in Eq. (8) are mixed; that is, each consists of both stresses and strains.

Eqs. (5) and (8) are the smearing relationships that define the micro-model. These relationships are also valid for *incremental stresses and strains*.

Tangent Stiffness

The tangent stiffness relates incremental (unit-cell-average) stresses and strains. The tangent stiffness for the unit cell is built up from tangent stiffness relations for the three components; These may be linear relationships or they may reflect various types of nonlinearities. Specific forms of nonlinear models are discussed later.

The relations between incremental stress and strain for the three material components of the unit cell are expressed directly in terms of tangent compliance matrices, and partitioned in accordance with Eq. (7), as

$$\begin{bmatrix} d\epsilon_a \\ d\epsilon_b \end{bmatrix} = \begin{bmatrix} S_{aa} & S_{ab} \\ S_{ba} & S_{bb} \end{bmatrix} \begin{bmatrix} d\sigma_a \\ d\sigma_b \end{bmatrix} \quad (9)$$

in which S is the tangent compliance matrix.

The tangent compliance matrix is now partially-inverted to provide relations of the form

$$\begin{bmatrix} d\sigma_a \\ d\epsilon_b \end{bmatrix} = \begin{bmatrix} A & B \\ -B^T & D \end{bmatrix} \begin{bmatrix} d\epsilon_a \\ d\sigma_b \end{bmatrix} \quad (10)$$

in which A is (1x1), B is (1x5), and D is (5x5), and are given by

$$\begin{aligned} A &= (1/S_{aa}) \\ B &= -(1/S_{aa}) \cdot S_{ab} \\ D &= S_{bb} - (1/S_{aa}) \cdot S_{ba} S_{ab} \end{aligned} \quad (11)$$

Thus the only "inversion" required is that of S_{aa} , a (1x1).

Material Element A

With the tangent relations expressed in the form of Eq. (10), the smearing relation Eq. (8) can be applied to give the partially-inverted tangent compliance for Material Element A as

$$\begin{bmatrix} d\sigma_a \\ d\epsilon_b \end{bmatrix}_A = \begin{bmatrix} A & B \\ -B^T & D \end{bmatrix}_A \begin{bmatrix} d\epsilon_a \\ d\sigma_b \end{bmatrix}_A \quad (12)$$

$$\begin{bmatrix} A & B \\ -B^T & D \end{bmatrix}_A \equiv \left(w_f \begin{bmatrix} A & B \\ -B^T & D \end{bmatrix}_f + w_m \begin{bmatrix} A & B \\ -B^T & D \end{bmatrix}_m \right)$$

The partial inversion is now completed to give the tangent stiffness for Material Element A as

$$\begin{bmatrix} d\sigma_a \\ d\sigma_b \end{bmatrix}_A = \begin{bmatrix} C_{aa} & C_{ab} \\ \text{---} & \text{---} \\ C_{ba} & C_{bb} \end{bmatrix}_A \begin{bmatrix} d\epsilon_a \\ d\epsilon_b \end{bmatrix}_A \quad (13)$$

in which

$$\begin{aligned} C_{bb} &= D^{-1} \\ C_{ab} &= B C_{bb} \\ C_{aa} &= A + C_{ab} B^T \end{aligned} \quad (14)$$

Material Element B

The tangent compliance matrix for Material Element B, which consists of a single matrix element, is inverted to give the tangent stiffness relation as

$$\begin{bmatrix} d\sigma_a \\ d\sigma_b \end{bmatrix}_B = \begin{bmatrix} C_{aa} & C_{ab} \\ \text{---} & \text{---} \\ C_{ba} & C_{bb} \end{bmatrix}_B \begin{bmatrix} d\epsilon_a \\ d\epsilon_b \end{bmatrix}_B \quad (15)$$

Unit Cell

The smearing relation Eq (5) is now applied to give the tangent stiffness relation for the unit cell as

$$\begin{bmatrix} d\sigma_a \\ d\sigma_b \end{bmatrix}_C = \begin{bmatrix} C_{aa} & C_{ab} \\ \text{---} & \text{---} \\ C_{ba} & C_{bb} \end{bmatrix}_C \begin{bmatrix} d\epsilon_a \\ d\epsilon_b \end{bmatrix}_C \quad (16)$$

$$\begin{bmatrix} C_{aa} & C_{ab} \\ \text{---} & \text{---} \\ C_{ba} & C_{bb} \end{bmatrix}_C \equiv \left(w_f \begin{bmatrix} C_{aa} & C_{ab} \\ \text{---} & \text{---} \\ C_{ba} & C_{bb} \end{bmatrix}_A + w_m \begin{bmatrix} C_{aa} & C_{ab} \\ \text{---} & \text{---} \\ C_{ba} & C_{bb} \end{bmatrix}_B \right)$$

Elastic Tangent Compliance

The elastic tangent compliance relations are an ingredient of any nonlinear model. These relations are expressed directly for each component in terms of engineering properties as follows

$$\begin{bmatrix} \epsilon_{11} \\ \epsilon_{22} \\ \gamma_{12} \\ \epsilon_{33} \\ \gamma_{23} \\ \gamma_{13} \end{bmatrix} = \begin{bmatrix} \frac{1}{E_1} & & & & & & \\ -\frac{\nu_{12}}{E_1} & \frac{1}{E_2} & & & & & \\ 0 & 0 & \frac{1}{G_{12}} & & & & \\ -\frac{\nu_{13}}{E_1} & -\frac{\nu_{23}}{E_2} & 0 & \frac{1}{E_3} & & & \\ 0 & 0 & 0 & 0 & \frac{1}{G_{23}} & & \\ 0 & 0 & 0 & 0 & 0 & \frac{1}{G_{13}} & \end{bmatrix} \begin{bmatrix} \sigma_{11} \\ \sigma_{22} \\ \tau_{12} \\ \sigma_{33} \\ \tau_{23} \\ \tau_{13} \end{bmatrix} \quad (17)$$

For transversely isotropic component materials,

$$\begin{aligned} E_2 &= E_3 & G_{12} &= G_{13} & \nu_{12} &= \nu_{13} \\ G_{23} &= \frac{E_2}{2(1 + \nu_{23})} \end{aligned} \quad (18)$$

so that there are 5 independent elastic constants.

For isotropic component materials,

$$\begin{aligned} E_1 &= E_2 = E_3 \equiv E \\ \nu_{12} &= \nu_{23} = \nu_{13} \equiv \nu \\ G_{12} &= G_{23} = G_{13} \equiv \frac{E}{2(1 + \nu)} \end{aligned} \quad (19)$$

4.2. Sublaminar Model

The sublaminar consists of the smallest typical repeating unit from which the laminate is constructed. For example, for a $[0_2/90]_{16}$ laminate, which consists of 96 plies, the sublaminar is $[0_2/90]$, i.e. 3 plies.

The sublaminar model provides information on the material behavior in a neighborhood of each material point in the structural model. In this neighborhood, the actual laminate is represented as an equivalent *homogeneous anisotropic* material.

Equivalent Continuum Modeling

Equivalent continuum modeling has been used successfully, not only in composites, but in many other areas of mechanics; literally hundreds of papers could be cited. For example, the analysis of bodies with regular patterns of perforations (Malkin 1952, Horvay 1952, O'Donnell 1973, Porowski and O'Donnell 1974, Slot and Branca 1974, Pecknold and Presswalla 1983) is closely related to micromechanical modeling of composites. An early work (Hrennikoff 1941), which could be considered as a forerunner of the finite element method, turned the process around; an elastic continuum was modeled for analysis as an assemblage of discrete bars.

In many cases, the actual material has a fine-grained microstructure which cannot, or need not, be explicitly treated in the analysis. Even though the basic components of the material at the microstructural level may exhibit isotropic behavior, the overall response may be anisotropic, because of this microstructure. The relation of the microstructure to the resulting elastic symmetry of the equivalent material is an interesting question which is apparently not completely resolved (Christensen 1987).

The philosophy of all of these methods is the same: for analysis, replace the actual material by a well-defined *equivalent* material; the properties of this equivalent material are determined by requiring that the actual and equivalent materials respond in the same way when subjected to certain *fundamental patterns* of stress or strain. These fundamental patterns should include spatially homogeneous conditions of stress and/or strain, but may include higher-order spatial variations as well, depending on the complexity of the postulated equivalent material.

Note that in the actual structure which is analyzed, the stress and strain conditions will generally be much more complex than these fundamental patterns. Thus, the modeling should be done in such a way that the variation of stress and strain over a material neighborhood is not "too large", so that the conditions experienced by the equivalent material are not too much different from the fundamental patterns with which it was calibrated.

In the sublaminar model proposed here, the equivalent material is homogeneous. If, for example, the laminate is made of only a few plies with greatly differing elastic properties from ply to ply, this approach must be expected to lose accuracy; ply-by-ply analysis may then be necessary. However, with only a few plies, it probably also is then feasible.

If, on the other hand, the laminate consists of a large number of plies (the case of interest), but stress and strain variations are large across its thickness, enough material points should be used through the thickness to reduce the size of the material neighborhood around a given material point. Then, the variation of stress and strain over a single neighborhood will not be large and the approach should be accurate.

Analysis of the equivalent material yields average or *nominal* stresses and strains; information on local stresses and strains at the microstructural level can only be recovered by back-calculating unit cell response to these nominal stresses and strains (Pecknold and Presswalla 1983).

The lamina micro-model described earlier, as well as all of the micromechanical models for composites, uses the general approach described above. The sublaminar model (Fig. 7) is also based on this approach and is described next.

Partitioning of Stress and Strain Vectors

The stress and strain vectors for each lamina from which the sublaminar is constructed are partitioned into *in-plane* and *out-of-plane* components.

$$\begin{bmatrix} \sigma \end{bmatrix} = \begin{bmatrix} \sigma_{11} \\ \sigma_{22} \\ \tau_{12} \\ \hline \sigma_{33} \\ \tau_{23} \\ \tau_{13} \end{bmatrix} \equiv \begin{bmatrix} \sigma_i \\ \hline \sigma_o \end{bmatrix} \quad \begin{bmatrix} \epsilon \end{bmatrix} = \begin{bmatrix} \epsilon_{11} \\ \epsilon_{22} \\ \gamma_{12} \\ \hline \epsilon_{33} \\ \gamma_{23} \\ \gamma_{13} \end{bmatrix} \equiv \begin{bmatrix} \epsilon_i \\ \hline \epsilon_o \end{bmatrix} \quad (20)$$

Note that the ordering of the stress and strain components is unchanged, but the partitioning is different than that used for the micro-model, Eq. (7).

Transformation to Global Coordinates

Some additional notation is now required to distinguish quantities referred to the lamina, or local, (1 2 3) coordinate system from those referred to the laminate, or global, (x y z) coordinate system, Fig. 7. σ' and ϵ' will now denote stresses and strains in a lamina coordinate system, and σ and ϵ will denote quantities referred to the laminate system. In addition, where needed for clarity, a superscript k will indicate a particular lamina. The transformation between local and global coordinates is

$$\begin{bmatrix} \epsilon' \end{bmatrix} = \begin{bmatrix} \mathbf{T} \end{bmatrix} \begin{bmatrix} \epsilon \end{bmatrix} \quad \begin{bmatrix} \sigma \end{bmatrix} = \begin{bmatrix} \mathbf{T} \end{bmatrix}^T \begin{bmatrix} \sigma' \end{bmatrix} \quad (21)$$

The transformations for in-plane and out-of plane stresses and strains uncouple

$$\mathbf{T} = \left[\begin{array}{c|c} \mathbf{T}_i & 0 \\ \hline 0 & \mathbf{T}_o \end{array} \right] \quad (22)$$

$$\mathbf{T}_i = \begin{bmatrix} c^2 & s^2 & s c \\ s^2 & c^2 & -s c \\ -2 s c & 2 s c & c^2 - s^2 \end{bmatrix} \quad \mathbf{T}_o = \begin{bmatrix} 1 & 0 & 0 \\ 0 & c & -s \\ 0 & s & c \end{bmatrix}$$

$$c \equiv \cos \alpha^k$$

$$s \equiv \sin \alpha^k$$

where α^k is the angle between the fiber direction (1) in lamina k and the global x axis.

Stress and Strain Smearing in Sublaminate

The interlaminar continuity conditions, Fig. 1, require that in-plane strains and out-of-plane stresses be continuous across interfaces.

Thus at the interface between lamina k and lamina $k+1$

$$\begin{bmatrix} \epsilon_i \\ \sigma_o \end{bmatrix}^k = \begin{bmatrix} \epsilon_i \\ \sigma_o \end{bmatrix}^{k+1} \quad (23)$$

Fundamental Patterns of Stress and Strain for Definition of Equivalent Material

The fundamental patterns of stress and strain which are used to define the equivalent material should include spatially homogeneous patterns. Higher order spatial variations could be used in addition, but they are not significant here because of the choice of a homogeneous continuum as the equivalent material.

The crucial step is to recognize that, in view of the interface conditions Eq. (23), the patterns that should be used are homogeneous *in-plane strains* and homogeneous *out-of-plane stresses*.

Thus for each lamina k

$$\begin{bmatrix} \epsilon_i \\ \sigma_o \end{bmatrix}^k = \begin{bmatrix} \bar{\epsilon}_i \\ \bar{\sigma}_o \end{bmatrix} \quad (24)$$

where the overbar indicates smeared sublaminate quantities.

Smeared In-plane Stresses and Out-of-plane Strains

The in-plane stresses and out-of-plane strains are now determined from

$$\begin{bmatrix} \bar{\sigma}_i \\ \bar{\epsilon}_o \end{bmatrix} = \sum_{k=1}^N \left(\frac{t^k}{t} \right) \begin{bmatrix} \sigma_i \\ \epsilon_o \end{bmatrix}^k \quad (25)$$

where t^k is the thickness of lamina k , t is the sublaminate thickness, and N is the number of laminae in the sublaminate.

Eqs. (24) and (25), which are analogous to Eq. (8) for the micro-model, characterize the sublaminate model. These relations also apply to incremental stresses and strains.

Tangent Stiffness

Incremental tangent stiffness relations for a lamina are given in Eq. (16). These are transformed to global coordinates to give

$$[d\sigma] = [C][d\epsilon] \quad (26)$$

$$[C] = [T]^T [C'] [T]$$

The lamina stiffness is now partially inverted to give

$$\begin{bmatrix} d\sigma_i \\ d\epsilon_o \end{bmatrix} = \begin{bmatrix} A & B \\ -B^T & D \end{bmatrix} \begin{bmatrix} d\epsilon_i \\ d\sigma_o \end{bmatrix} \quad (27)$$

in which

$$\begin{aligned}
\mathbf{D} &= \mathbf{C}_{oo}^{-1} \\
\mathbf{B} &= \mathbf{C}_{lo} \cdot \mathbf{D} \\
\mathbf{A} &= \mathbf{C}_{ll} - \mathbf{B} \cdot \mathbf{C}_{ol}
\end{aligned}
\tag{28}$$

The sublaminar smearing gives

$$\begin{bmatrix} d\bar{\sigma}_l \\ d\bar{\sigma}_o \end{bmatrix} = \begin{bmatrix} \bar{\mathbf{A}} & \bar{\mathbf{F}} \\ -\bar{\mathbf{B}}^T & \bar{\mathbf{D}} \end{bmatrix} \begin{bmatrix} d\bar{\epsilon}_l \\ d\bar{\epsilon}_o \end{bmatrix}
\tag{29}$$

$$\begin{bmatrix} \bar{\mathbf{A}} & \bar{\mathbf{B}} \\ -\bar{\mathbf{B}}^T & \bar{\mathbf{D}} \end{bmatrix} = \sum_{k=1}^N \left(\frac{t^k}{t} \right) \begin{bmatrix} \mathbf{A} & \mathbf{B} \\ -\mathbf{B}^T & \mathbf{D} \end{bmatrix}^k$$

The sublaminar tangent stiffness is then calculated from

$$\begin{bmatrix} d\bar{\sigma}_l \\ d\bar{\sigma}_o \end{bmatrix} = \begin{bmatrix} \bar{\mathbf{C}}_u & \bar{\mathbf{C}}_{lo} \\ \bar{\mathbf{C}}_{ol} & \bar{\mathbf{C}}_{oo} \end{bmatrix} \begin{bmatrix} d\bar{\epsilon}_l \\ d\bar{\epsilon}_o \end{bmatrix}
\tag{30}$$

$$\begin{aligned}
\bar{\mathbf{C}}_{oo} &= \bar{\mathbf{D}}^{-1} \\
\bar{\mathbf{C}}_{lo} &= \bar{\mathbf{B}} \cdot \bar{\mathbf{C}}_{oo} \\
\bar{\mathbf{C}}_{ol} &= \bar{\mathbf{C}}_{lo}^T \\
\bar{\mathbf{C}}_u &= \bar{\mathbf{A}} + \bar{\mathbf{C}}_{lo} \cdot \bar{\mathbf{B}}^T
\end{aligned}$$

Stress Updates

Stress updating is the most important task performed by the material model and, as already observed, it must be efficient because it is done so frequently. The stress update procedure for the thick-section material model will be more complex than for, say, a metal plasticity material model; this is a direct result of the two-level "microstructure" which is built into the thick-section model but hidden from the element and structural level processes.

In a standard nonlinear solution the material model receives increments of stress and strain $d\bar{\sigma}$, $d\bar{\epsilon}$ from the element processor. Strains are updated directly, i.e.

$$\bar{\epsilon} \leftarrow \bar{\epsilon} + d\bar{\epsilon} \quad (31)$$

However, material point stresses are not usually updated by $\bar{\sigma} \leftarrow \bar{\sigma} + d\bar{\sigma}$ since that would produce a cumulative error as indicated in Fig. 8, which would require quite small solution step sizes to control. Note that Fig. 8 should not be interpreted in too literal a sense, since in many cases, e.g. multi-axial incremental plasticity, an explicit relation $\bar{\sigma} = \bar{\sigma}(\bar{\epsilon})$ does not exist.

In the thick-section material model, stress and strain increments in all components can be back-calculated using tangent material properties. New stress and strain totals calculated from these tangential approximations satisfy all the equilibrium and compatibility relations (Eqs.(5),(8),(24) and (25)) which define the microstructure of the material model; however, these new totals will not satisfy nonlinear constitutive relations for the fiber and matrix elements of the lamina micro-model.

The basic approach in updating the stresses is to adjust the new totals so that the constitutive relations of the fiber and matrix elements, together with the microstructure relations, Eqs.(5),(8),(24) and (25), are satisfied to a specified tolerance; at the end of this process the smeared sublaminar strains $\bar{\epsilon} + d\bar{\epsilon}$ must be unchanged, and the updated stresses $\bar{\sigma}$ are delivered. From these updated stresses the internal force vector Eq.(3) can be determined.

Thus an iterative procedure is required, in which, for example, the out-of-plane strains of individual laminae can be adjusted, as long as their weighted-average is unchanged, i.e.

$$\sum_{k=1}^N \left(\frac{t^k}{t} \right) [\epsilon_o]^k = [\bar{\epsilon}_o] \quad (32)$$

There are many options available; further work is needed to develop an efficient stress update algorithm.

Comments on Related Work

Two previous works (Pagano 1974, Sun and Li 1988) utilize the same basic ideas for defining the equivalent elastic properties of the sublaminar. The presentation and viewpoint in these papers seem, to the author, to obscure the essential simplicity of the ideas involved, and has perhaps contributed to the situation where it was recently observed (Christensen 1988) that "two-dimensional lamination theory cannot be easily extended to three-dimensions". The sublaminar model presented here is a 3D lamination theory which is not much more complicated than CLT for two-dimensions.

5. Evaluation of Model Architecture

The proposed class of models has two essential components:

- 1) The lamina micro-model, Eqs. (5) and (8), and
- 2) The sublamine model, Eqs. (24) and (25).

In this section, the potential of the model is explored by examining its performance (1) in the elastic range and (2) using exact, rather than finite element, stress analysis at the structural level.

The intent is to separate issues of material–nonlinearity–modeling and stress analysis accuracy from issues of model architecture. Further, the lamina micro-model is evaluated independently from the sublamine model.

5.1. Lamina Micro-Model

Two sets of comparisons are made for the unit cell/lamina micro-model portion of the model: a comparison with results of detailed finite element micromodeling; and comparisons with experimental results.

Comparison with detailed FE Micromodeling

Equivalent elastic properties of a unidirectional graphite/epoxy lamina with a hexagonal fiber array were determined by detailed finite element micromodeling by Chen and Cheng (1970). Behrens (1971) compared these results with several simplified analytical models (Hashin and Rosen 1964, Hermans 1967, Whitney 1967).

The lamina properties were determined using the lamina micro-model, over the full range of fiber volume fraction, using the graphite and epoxy properties from Chen and Cheng (1970) shown in Table 1. Graphite fiber properties are transversely isotropic and the epoxy resin is isotropic.

The lamina transverse moduli E_2 and G_{12} are the most difficult to predict. For these engineering properties, Fig. 9 compares lamina micro-model values with the finite element results of Chen and Cheng. The lamina micro-model gives excellent results for this case.

In order to see if the lamina micro-model could be further simplified, the calculations were repeated using a simpler version, one consisting only of Material Element A (with the model weighting factors appropriately adjusted). Fig. 10 indicates that the results are then significantly less accurate, especially in the important mid-range of fiber volume fraction.

Comparison with DTRC Compression Test Results for Unidirectional Lamina

In an ongoing program at DTRC concerned with behavior of thick sections in compression, Camponeschi (1989a,b) determined unidirectional properties for AS4/3501-6 and S2 glass/3501-6 prepreg tapes using $[90]_{96}$ laminates.

The lamina micro-model was used to "predict" the prepreg tape properties from assumed constituent properties. Reasonable fiber and matrix properties were selected for this purpose (Table 2).

The micro-model results are shown in Tables 3 and 4. The lamina properties are predicted quite well; better fit with the experimental values can be achieved by tuning the constituent properties. Note that some constituent properties are often inferred in this way because they are difficult to measure directly.

5.2. Sublaminate Model

The sublaminate model was explored in two ways: first, comparisons were made with compression test results for $[0_2/90]_{16}$ laminates; second, exact elasticity solutions for thick cylinders under compression and bending were used to evaluate the sublaminate smearing procedure.

Comparison with DTRC Compression Test Results for Thick Laminate

In order to uncouple the sublaminate model from the lamina micro-model for evaluation purposes, the experimentally determined lamina properties for the AS4/3501-6 and S2 glass/3501-6 prepreg tapes (Table 3) were used in the sublaminate model to predict the equivalent-material properties of the 96-ply laminate.

Initial elastic properties determined from compression tests on 0.5-in thick $[0_2/90]_{16}$ laminates (Camponeschi 1989 a,b) are shown in Table 5, along with the sublaminate model results. These numerical results are identical to those that would be obtained by the procedures of Pagano (1974) or Sun and Li (1988).

Structural Analysis of Thick Cylinder

A model thick-walled cylinder (Fig. 11), with approximately the same dimensions as those tested at DTRC Carderock (Garala 1987), was analyzed using an exact elasticity solution for cross-ply laminated cylinders (Rahman 1990). This solution assumes a condition of plane strain in the cylinder axis direction, so there is no axial bending.

A general circumferentially-varying pressure load on the cylinder can be decomposed into its harmonic components, i.e. $p(\theta) = p_0 + \sum_n p_n \cos n\theta$. The axisymmetric pressure p_0

produces primarily a compressive mode of response in the cylinder wall; the ovalling pressure $p_2 \cos 2\theta$ produces primarily circumferential flexure. These two pressure distributions were selected as representative loading cases, with $p_0 = 10,000$ psi, and $p_2 = 100$ psi (Fig. 11). (Note that the load $p_1 \cos \theta$ cannot be treated by this particular plane-strain solution because it produces axial bending in the cylinder.)

The cylinder OD is 8.25 in.; the wall thickness is 0.48 in. The wall is assumed to be built up from 96 plies of AS4/3501-6 prepreg tape with the properties determined experimentally by Camponeschi (1989 a,b) shown in Table 3. Two different stacking sequences are considered: (1) $[0_2/90]_{16}$; and (2) $[0_{32}/90_{16}]$, which can be considered as a $[0_2/90]$ lay-up with ply thickness = $16 \times .005$ in. = .08 in. This latter designation will be used.

Response of $[0_2/90]_{16}$ Layup

This wall construction consists of 96 plies, each .005 in. thick, with two unidirectional plies in the circumferential direction for each one in the axial direction. This is the type of thick-section construction which is of primary interest; that is, many thin plies interleaved to produce an effectively homogeneous wall structure.

Figs. 12(a) and 12(b) show the through-thickness distributions of stress and strain for the axi-symmetric compressive response; Figs. 13(a) and 13(b) show the bending response. These responses, which were computed on a ply-by-ply basis from the exact elasticity solution, provide a standard of comparison for the sublaminated model.

First, some *general characteristics of the exact responses* should be noted in Figs. 12 and 13:

- (1) the in-plane strain ϵ_r and out-of-plane stresses σ_z and τ_{rz} (Figs. 12(a) and 13(a)) are not only continuous across ply interfaces, but are very smooth through the entire thickness;
- (2) the in-plane stress σ_r and out-of-plane strains ϵ_z and γ_{rz} (Figs. 12(b) and 13(b)) vary markedly from ply to ply (when there is an abrupt change of material properties), yet the distribution for each family of plies with the same orientation is smooth, forming, in this case, two envelopes of response. *Suppose that only the smoothly-varying responses ϵ_r , σ_z , τ_{rz} were known; the responses σ_r , ϵ_z , γ_{rz} which vary discontinuously from ply to ply could be easily, and exactly, calculated using individual ply properties.*

This latter observation bears directly on the evaluation of the sublaminated model. Figs. 12 and 13 show (superimposed on the exact responses) the responses computed from the smeared properties provided by the sublaminated model; i.e. the response of a homogeneous anisotropic cylinder with equivalent properties. The smoothly-varying responses ϵ_r , σ_z , τ_{rz} delivered by the sublaminated model are almost indistinguishable from those of the exact ply-by-ply analysis; this is the crucial result, because it follows that the remaining responses σ_r , ϵ_z , γ_{rz} can then be back-calculated easily and accurately from this information.

It is also of interest to examine the smeared responses $\bar{\sigma}_\theta$, $\bar{\epsilon}_r$, $\bar{\gamma}_{r\theta}$ from the sublaminar model although they are not directly used to determine corresponding ply values, as noted above. It is apparent from Figs. 12 and 13 that these smeared values are indeed weighted averages of the actual distributions.

These comparisons show that the sublaminar model is capable of producing very accurate responses.

Response of $[0_2/90]_r$ Layup

The $[0_2/90]_{16s}$ layup examined in the last section was idealized, in the stress analysis phase, as a homogeneous material through the thickness of the laminate; that is, the smeared elastic properties were used together with the exact solution for a single ply. In that case, a large number (32) of sublaminae constitute the laminate, and the variation of stress and strain over a single sublaminar is not large. Thus the idealization is accurate.

Now consider the $[0_2/90]_r$ layup shown in Figs. 14 and 15. Effectively, this wall construction consists of just 3 plies, each 0.16 in. thick; there are unidirectional circumferential plies at the inner and outer surfaces of the cylinder, and a single axial ply sandwiched between them. Assuming this layup to be homogeneous through the thickness will obviously underestimate the actual flexural stiffness of the section, which has circumferentially stiff layers at the outer fibers. Thus ϵ_θ is over-estimated (flexural stiffness too low) in bending (Fig. 15(a)), although it is still determined accurately in compression.

There are two alternatives here: treat the wall as piecewise homogeneous (if the analysis is done via finite element then use more than one element through-thickness); or, use shell theory rather than continuum modeling, in which flexural stiffness can be specified independently from membrane stiffness. In the latter case, the sublaminar model can be made to provide the necessary stiffness information by expanding the set of fundamental patterns of stress and strain to include in-plane strains which vary linearly in the thickness direction (Pagano 1974).

In the case of finite element modeling, special techniques can be used to enforce inter-laminar stress continuity within the framework of conventional displacement-based methods (Rahman 1990).

6. Nonlinearities

The modeling of several different types of nonlinear behavior and associated failure modes (Chou et al 1986) are of particular interest and importance for the structural analysis of laminated composites.

(a) *Kink-banding* is the dominant failure mode of laminates in direct compression (Camponeschi 1989 a,b); similar behavior is observed in other materials having a laminated structure such as wood (Wilson et al 1979) and rock (Donath 1970). The underlying mechanism is fiber micro-buckling, which is sensitive to fiber-matrix interaction and imperfections such as fiber waviness (Davis 1975). The phenomenon has been known for some time; Orowan (1942) refers to earlier work dating to 1898. However, much of the literature is descriptive and qualitative. Simple analytical formulae are available (Argon 1972, Evans and Adler 1978, Budiansky 1983) but these do not correlate well with experimental failure loads. A general analytical approach is apparently not yet available.

(b) *Interply delamination* is a frequently observed failure mode in thin laminates, particularly in bending or in bending-direct stress combinations. Local delaminations may couple with global stability behavior in composite shells, by reducing stiffness locally; similarly, delamination is associated with, and may interact with, kink-band failure modes (Camponeschi 1989).

(b) *Matrix nonlinearity* in epoxy resins is well-known (Adams 1974) and is most pronounced in pure shear. A degrading shear modulus can have an important detrimental influence on the global stability behavior of composite shells. Furthermore, softening of the matrix in shear may interact with kink-banding; the simple analytical formulae (Budiansky 1983) that predict kink-band failure stresses show that the matrix shear modulus is the dominant parameter.

Modeling Approaches

Nonlinear behavior can be introduced into the proposed material model in several ways:

- (1) in the constitutive models for the fiber and matrix elements;
- (2) in the coupling between fiber and matrix elements in the lamina micro-model; and
- (3) in the coupling between laminae in the sublaminar model.

Even though kink-banding is a stability-related phenomenon on the micro-scale, it may be possible to model it as a material nonlinearity in the fiber constitutive model. Modeling of local buckling phenomena as material nonlinearities has been successful in structural analyses with other materials.

An approach for modeling interply delamination is to interpose a thin layer with degrading tensile strength between laminae in the sublaminar model; an alternate approach is to introduce this behavior directly into the matrix constitutive model.

Modeling of matrix nonlinearity can be done via the matrix element constitutive model. Plasticity-based formulations are feasible (Adams 1974, Pindera et al 1990, Aboudi 1990); but nonlinear elastic models provide a simpler alternative.

Nonlinear Elastic Model for Matrix

Compression tests at DTRC (Camponeschi 1989a,b) indicate that the nonlinear response of thick laminates is essentially reversible over a substantial loading range. With this in mind, a nonlinear elastic model is proposed as a reasonable first step in modeling matrix nonlinearities in thick-section laminates.

The primary effect which is observed is nonlinear softening in pure shear. This can be modeled by a power-law relation

$$\gamma = \frac{\tau}{G} + \beta \frac{\tau_0}{G} \left(\frac{\tau}{\tau_0} \right)^n \quad (33)$$

where β , τ_0 , and n are material constants to be determined.

In addition, a nonlinear pressure-volume change response can be modeled by a similar power-law relation as

$$\theta = \frac{p}{K} + \alpha \frac{p_0}{K} \left(\frac{p}{p_0} \right)^m \quad (34)$$

in which p is the hydrostatic pressure, θ is the volume change, $K \equiv \frac{E}{3(1-2\nu)}$ is the elastic bulk modulus and α , p_0 , and m are material constants to be determined.

Pressure-volume change nonlinearities in the matrix are probably of minor importance, but are included here for generality.

These two power-law relations must be stated in a form which is valid for general multi-axial stress states, i.e.

$$\epsilon_{ij} = \epsilon_{ij}^e + \frac{\alpha}{3K} \left(\frac{p_e}{p_0} \right)^{m-1} p \delta_{ij} + \frac{\beta}{2G} \left(\frac{\tau_e}{\tau_0} \right)^{n-1} s_{ij} \quad (35)$$

in which ϵ_{ij}^e are linear elastic strains and

$$\begin{aligned} p &\equiv \frac{1}{3} \sigma_{kk} & s_{ij} &\equiv \sigma_{ij} - p \delta_{ij} \\ p_e &\equiv |p| & \tau_e &\equiv \sqrt{\frac{1}{2} s_{ij} s_{ij}} \end{aligned} \quad (36)$$

The incremental form of Eq. (35) is

$$\begin{aligned} d\epsilon_{ij} = d\epsilon_{ij}^e + \frac{a}{3K} m \left(\frac{p_e}{p_0} \right)^{m-1} dp \delta_{ij} + \frac{\beta}{2G} \left(\frac{\tau_e}{\tau_0} \right)^{n-1} ds_{ij} \\ + \frac{\beta}{2G} \frac{n-1}{2} \left(\frac{\tau_e}{\tau_0} \right)^{n-1} \bar{s}_{ij} \bar{s}_{kl} ds_{kl} \end{aligned} \quad (37)$$

where the normalized deviator stresses are

$$\bar{s}_{ij} \equiv \frac{s_{ij}}{\tau_e} \quad (38)$$

Eqs. (35) and (37) can be expressed in matrix form as

$$[\epsilon] = \left[c_1 [S_1] + c_2 [S_2] \right] [\sigma] \quad (39)$$

and

$$[d\epsilon] = \left[d_1 [S_1] + d_2 [S_2] + d_3 [S_3] \right] [d\sigma] \quad (40)$$

where the stress and strain vectors are ordered as in Eq. (20), the matrices S_1, S_2, S_3 are

$$[S_1] = \begin{bmatrix} 1 & & & & & & \\ 1 & 1 & & & & & \\ 0 & 0 & 0 & & & & \\ 1 & 1 & 0 & 1 & & & \\ 0 & 0 & 0 & 0 & 0 & & \\ 0 & 0 & 0 & 0 & 0 & 0 & \end{bmatrix} \quad [S_2] = \begin{bmatrix} 1 & & & & & & \\ 0 & 1 & & & & & \\ 0 & 0 & 2 & & & & \\ 0 & 0 & 0 & 1 & & & \\ 0 & 0 & 0 & 0 & 2 & & \\ 0 & 0 & 0 & 0 & 0 & 2 & \end{bmatrix}$$

(41)

$$[S_3] = \bar{s} \bar{s}^T \quad \bar{s} = \begin{bmatrix} \bar{s}_{11} \\ \bar{s}_{22} \\ 2\bar{s}_{12} \\ \bar{s}_{33} \\ 2\bar{s}_{23} \\ 2\bar{s}_{13} \end{bmatrix}$$

and the functions c_1 , c_2 and d_1 , d_2 , d_3 are given by

$$c_1 = \left[\frac{1}{9K} (1+a) - \frac{1}{6G} (1+b) \right]$$

$$c_2 = \left[\frac{1}{2G} (1+b) \right]$$

$$d_1 = \left[\frac{1}{9K} (1+m a) - \frac{1}{6G} (1+b) \right]$$

$$d_2 = c_2$$

$$d_3 = \left[\frac{1}{2G} \frac{n-1}{2} b \right]$$

(42)

$$a \equiv a \left(\frac{p_e}{p_0} \right)^{n-1}$$

$$b \equiv \beta \left(\frac{\tau_e}{\tau_0} \right)^{n-1}$$

Eq. (40) gives the nonlinear tangent compliance matrix for the matrix elements in the lamina micro-model. The material constants can be determined by fitting lamina micro-model response to finite element micromechanical results (WYO2D) or to experimental

results. A parameter value $\alpha = 0$ removes the pressure-volume change nonlinearity; and a value $\beta = 1$ provides sufficient generality for modeling the shear behavior. Good initial estimates for τ_0 and n can be obtained from neat resin response data; final values of n should be somewhat lower (more gradual softening) since the lamina micro-model deals with average stresses rather than local stresses.

7. Summary and Conclusions

The material model architecture which has been developed has several attractive features:

- 1) It presents a standard interface to structural analysis packages. The material model micro-structure is hidden from the element and structural-level processes.
- 2) It is simple enough to be a viable approach for nonlinear structural analysis.
- 3) It is based on simplified micro-mechanical analysis, and allows predictions of material and structural behavior to be made, starting from known or assumed material properties for fiber and matrix constituents.
- 4) It is accurate, as shown by comparisons with experiments, detailed finite element micromechanical results, and ply-by-ply elasticity solutions for a thick cylinder.
- 5) The model architecture provides sufficient flexibility for modeling different types of nonlinear behavior.

8. Development Plan

A plan for developing the material modeling capability is:

(1) Implement the material model with the simple power-law nonlinearity for the matrix; and with *tangential stress updates*, i.e. $\bar{\sigma} \leftarrow \bar{\sigma} + d\bar{\sigma}$. This is a simple initial version of the material model with a crude stress updating procedure.

(2) The development now follows two parallel paths:

(A) Carry out nonlinear structural analyses of stiffened and unstiffened composite shells, including stability effects. This serves two purposes: first, an early indication is provided of the potential importance of nonlinear material behavior for *structural response*; and, second, important experience will be obtained to guide further material model development.

(B) Couple the initial version of the material model to a material model driver, which mimics the structural package interface and allows the material model to be exercised over arbitrary stress and strain histories.

(i) Carry out comparisons with micromechanical analyses, DTRC thick-section compression tests, and results available in the literature to determine material model parameters for the power-law model. Incorporate this information in structural analysis studies, Part(A).

(ii) If initial evaluations are favorable, continue development of material model: develop and implement stress-update algorithm; investigate kink-banding and interply delamination modeling issues.

9. References

- [1]Aboudi, J. 1990. The nonlinear behavior of unidirectional and laminated composites -- a micromechanical approach, *J. Reinforced Plastics and Composites*, 9(1), 13-32.
- [2]Adams, D. 1974. Elastoplastic behavior of composites, Chapter 5 in *Mechanics of Composite Materials* G. P. Sendeckyj (Ed.), Academic Press, 169-208.
- [3]Argon, A.S. 1972. *Treatise on Materials Science and Technology*, Vol. 1, Academic Press, 79.
- [4]Behrens, E. 1971. Elastic constants of fiber-reinforced composites with transversely isotropic constituents, *J. Appl. Mech.*, 38(12), 1062-1065.
- [5]Budiansky, B. 1983. Micromechanics, *Comput. Structures*, 16(1-4), 3-12.
- [6]Camponeschi, E.T. Jr. 1987. Compression of composite materials -- a review, David Taylor Research Center, Bethesda, MD, DTRC-87/050, 54 pp.
- [7]Camponeschi, E.T. Jr. 1989a. Through-thickness strain response of thick composites in compression, David Taylor Research Center, Bethesda, MD, DTRC-SME-89/67, 30 pp.
- [8]Camponeschi, E.T. Jr. 1989b. Compression testing of thick-section composite materials, David Taylor Research Center, Bethesda, MD, DTRC-SME-89/73, 31 pp.
- [9]Chen, C.H. and Cheng S. 1970. Mechanical properties of anisotropic fiber-reinforced composites, *J. Appl. Mech.*, 37(3), 186-189.
- [10]Chou, T-W., McCullough, R.L. and Pipes, R.B. 1986. Composites, *Scientific American*, (10), 193-203.
- [11]Christensen, R.M. 1987. Sufficient symmetry conditions for isotropy of the elastic moduli tensor, *J. Appl. Mech.*, 54(12), 772-777.
- [12]Christensen, R.M. 1988. Tensor transformations and failure criteria for the analysis of fiber composite materials, *J. Composite Materials*, 22(9), 874-897.
- [13]Davis, J.G. Jr. 1975. Compressive strength of fiber-reinforced composite materials, *Composite Reliability*, ASTM STP 580, American Society for Testing and Materials, 364-377.
- [14]Donath, F.A. 1970. Some information squeezed out of rock, *American Scientist*, 58(1), 54-72.
- [15]Evans, A.G. and Adler, W.F. 1978. Kinking as a mode of structural degradation in carbon fiber composites, *Acta Metallurgica*, 26, 725-738.
- [16]Garala, H.J. 1987. Experimental evaluation of graphite/epoxy composite cylinders subjected to external hydrostatic compressive loading, *Proc. of 1987 Spring Conference on Experimental Mechanics*, Society for Experimental Mechanics, 948-951.

- [17]Hashin, Z. and Rosen, B.W. 1964. The elastic moduli of fiber reinforced materials, *J. Appl. Mech.*, 31(), 223-
- [18]Hashin, Z., Bagchi, D. and Rosen, B.W. 1974. Non-linear behavior of fiber composite laminates, NASA Contractor Report, NASA CR-2313, 130 pp.
- [19]Hermans, J.J. 1967. The elastic properties of fiber-reinforced materials when the fibers are aligned. *Proc. Royal Acad., Amsterdam. Ser. B* (70), 1-9.
- [20]Horvay, G. 1952. The plane-stress problem of perforated plates, *J. Appl. Mech.*, 19, 355-360.
- [21]Hrennikoff, A. 1941. Solution of problems in elasticity by the framework method, *J. Appl. Mech.*, 8(), 169-175.
- [22]Malkin, I. 1952. Notes on a theoretical basis for design of tube sheets of triangular layout, *Trans. ASME*, 74, 387-396.
- [23]O'Donnell, W.J. 1973. Effective elastic constants for the bending of thin perforated plates with triangular and square penetration patterns, *J. Engng. Ind. ASME*, 95, 121-128.
- [24]Orowan, E. 1942. A type of plastic deformation new in metals, *Nature*, 149, 643-644.
- [25]Pagano, N.J. 1974. Exact moduli of anisotropic laminates, Chapter 2 in *Mechanics of Composite Materials* G. P. Sendeckyj (Ed.), Academic Press, 23-44.
- [26]Pecknold, D.A. and Presswalla, H. 1983. Elastoplastic analysis of thick perforated plates with application to prestressing anchor heads, *Comput. Structures*, 17(4), 539-553.
- [27]Pindera, M-J., Herakovich, C. T., Becker, W. and Aboudi, J. 1990. Nonlinear response of unidirectional boron/aluminum, *J. Composite Materials*, 24(1), 2-21.
- [28]Porowski, J. and O'Donnell, W.J. 1974. Effective plastic constants for perforated materials, *J. Pressure Vessel Tech. ASME*, 96, 234-241.
- [29]Rahman, S, 1990. A solid element for the analysis of thick-section composites. Unpublished Ph. D. thesis proposal, Univ. of Illinois.
- [30]Slot, T. and Branca, T.R. 1974. On the determination of effective elastic-plastic constants for the equivalent solid plate analysis of tube sheets, *J. Pressure Vessel Tech. ASME*, 96, 220-227.
- [31]Sun, C.T. and Li, S. 1988. Three-dimensional effective elastic constants for thick laminates, *J. Composite Materials*, 22(7), 629-639.
- [32]Whitney, J.M. 1967. Elastic moduli of unidirectional composites with anisotropic filaments, *J. Composite Materials*, 1(), 188-193.
- [33]Wilson, J.B., McEvoy, R.P. and Perkins, R.W. 1979. On compression failure in wood materials: a mathematical and experimental simulation, *Proc. of the First International Conference on Wood Fracture*, Forintek Canada Corp., 290-301.

	Graphite	Epoxy	
E_1	$24 \times 10^6 \text{ psi}$	$0.6 \times 10^6 \text{ psi}$	E
E_2	$2 \times 10^6 \text{ psi}$		
G_{12}	$4 \times 10^6 \text{ psi}$		
ν_{12}	0.30	0.30	ν
ν_{23}	0.15		

Table 1. Graphite and Epoxy Properties used in comparisons with FE micromechanical modeling

	AS4 Carbon Fibers	S2 glass Fibers	3501-6 Epoxy	
E_1	$27 \times 10^6 \text{ psi}$	$12.6 \times 10^6 \text{ psi}$		E
E_2	$2.5 \times 10^6 \text{ psi}$			
G_{12}	$5 \times 10^6 \text{ psi}$		$0.26 \times 10^6 \text{ psi}$	G
ν_{12}	0.30	0.25	0.40	ν
ν_{23}	0.25			

Table 2. Fiber and Matrix Properties used for prediction of Lamina Properties

AS4 / 3501-6 prepreg FVF = 60 %

	<i>Experimental</i>	<i>Micro-Model</i>
E_1	$16.48 \times 10^6 \text{ psi}$	$16.50 \times 10^6 \text{ psi}$
E_2	$1.40 \times 10^6 \text{ psi}$	$1.56 \times 10^6 \text{ psi}$
E_3	$1.40 \times 10^6 \text{ psi}$	$1.56 \times 10^6 \text{ psi}$
ν_{12}	0.334	0.337
ν_{13}	0.328	0.337
ν_{23}	0.540	0.468
G_{12}	¹ $0.87 \times 10^6 \text{ psi}$	$0.82 \times 10^6 \text{ psi}$
G_{13}	² $0.87 \times 10^6 \text{ psi}$	$0.82 \times 10^6 \text{ psi}$
G_{23}	³ $0.55 \times 10^6 \text{ psi}$	$0.53 \times 10^6 \text{ psi}$

- Notes : 1 $[\pm 45]_2$ tension test
 2 G_{13} assumed equal to G_{12}
 3 G_{23} from literature

Table 3. Lamina Properties for AS4/3501-6 Prepreg Tape

S2 glass / 3501-6 prepreg FVF = 54 %

	<i>Experimental</i>	<i>Micro-Model</i>
E_1	$7.15 \times 10^6 \text{ psi}$	$7.15 \times 10^6 \text{ psi}$
E_2	$2.13 \times 10^6 \text{ psi}$	$2.21 \times 10^6 \text{ psi}$
E_3	$2.13 \times 10^6 \text{ psi}$	$2.21 \times 10^6 \text{ psi}$
ν_{12}	0.296	0.302
ν_{13}	0.306	0.302
ν_{23}	0.499	0.576
G_{12}	¹ $0.98 \times 10^6 \text{ psi}$	$0.70 \times 10^6 \text{ psi}$
G_{13}	² $0.98 \times 10^6 \text{ psi}$	$0.70 \times 10^6 \text{ psi}$
G_{23}	³ $0.55 \times 10^6 \text{ psi}$	$0.70 \times 10^6 \text{ psi}$

- Notes :
- 1 $[\pm 45]_2$ tension test
 - 2 G_{13} assumed equal to G_{12}
 - 3 G_{23} from literature

Table 4. Lamina Properties for S2 glass/3501-6 Prepreg Tape

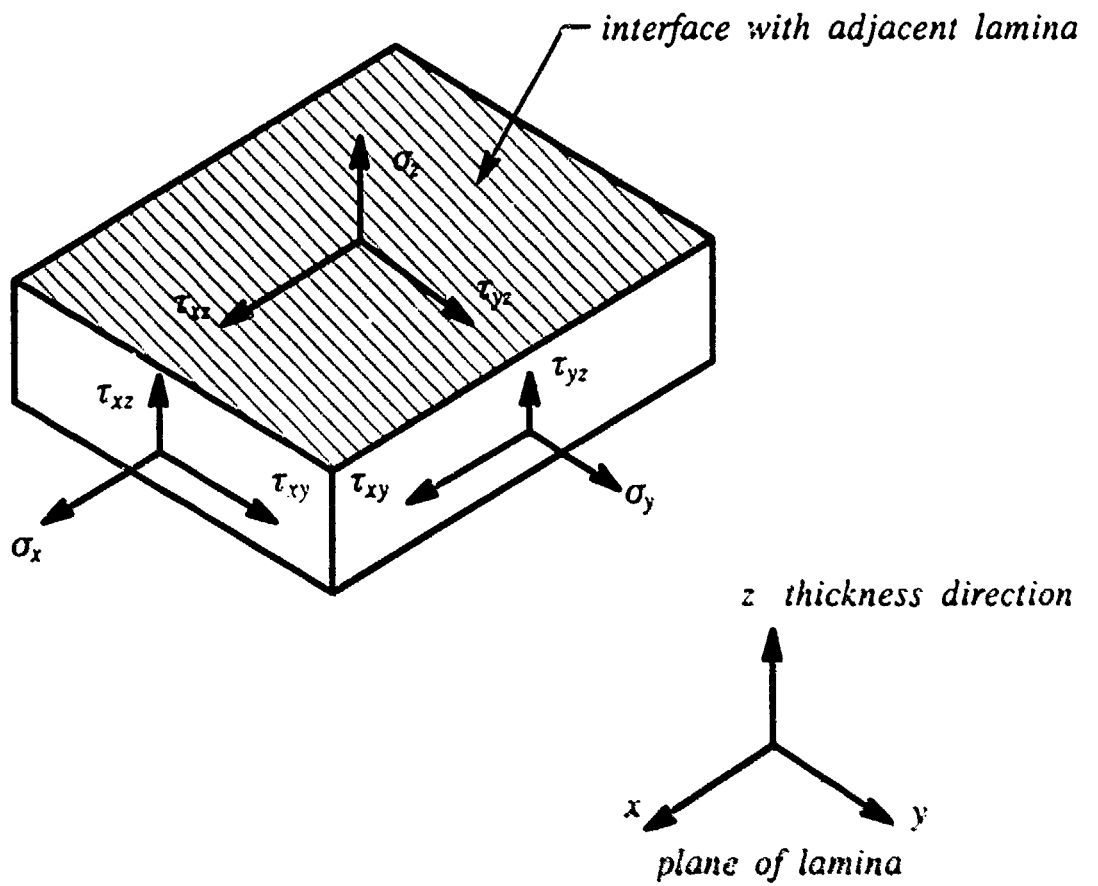
[0₂ / 90]_{16s} Laminate

Carbon / Epoxy

S2 glass / Epoxy

	Experimental	Sublamine Model	Experimental	Sublamine Model
E_x	$11.63 \times 10^6 \text{ psi}$	$11.53 \times 10^6 \text{ psi}$	$5.82 \times 10^6 \text{ psi}$	$5.52 \times 10^6 \text{ psi}$
E_y		$6.47 \times 10^6 \text{ psi}$		$3.83 \times 10^6 \text{ psi}$
E_z		$1.80 \times 10^6 \text{ psi}$		$2.38 \times 10^6 \text{ psi}$
ν_{xy}	0.069	0.073	0.166	0.166
ν_{xz}	0.469	0.488	0.363	0.405
ν_{yz}		0.519		0.459
G_{xy}		$0.87 \times 10^6 \text{ psi}$		$0.98 \times 10^6 \text{ psi}$
G_{xz}		$0.73 \times 10^6 \text{ psi}$		$0.78 \times 10^6 \text{ psi}$
G_{yz}		$0.63 \times 10^6 \text{ psi}$		$0.64 \times 10^6 \text{ psi}$

Table 5. Smearred Properties for 96-ply Laminates



Interface Conditions

Continuity of In-plane Strains	$\epsilon_x, \epsilon_y, \gamma_{xy}$
& Out-of-Plane Stresses	$\sigma_z, \tau_{yz}, \tau_{xz}$

Fig. 1 Interface Conditions between adjacent Laminae

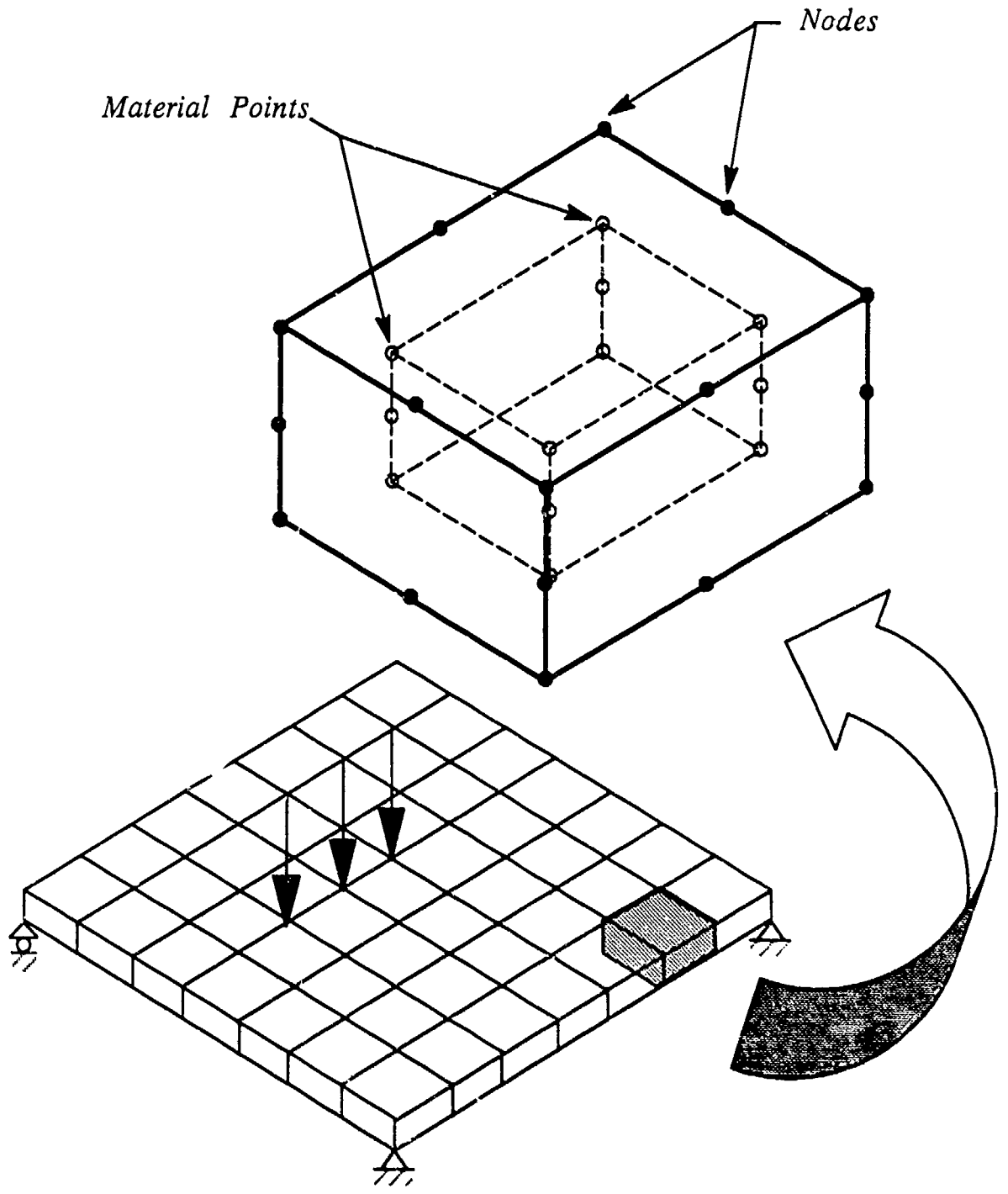


Fig. 2 Material Points (Gauss Integration Points) for Tracking Material Response

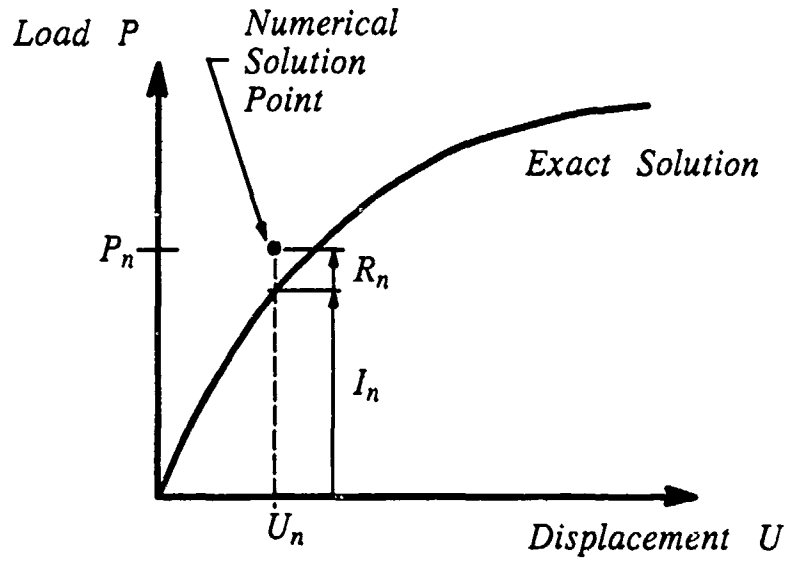


Fig. 3 Numerical Solution of Nonlinear Structural Equations; Illustrating Internal Force I and Residual R

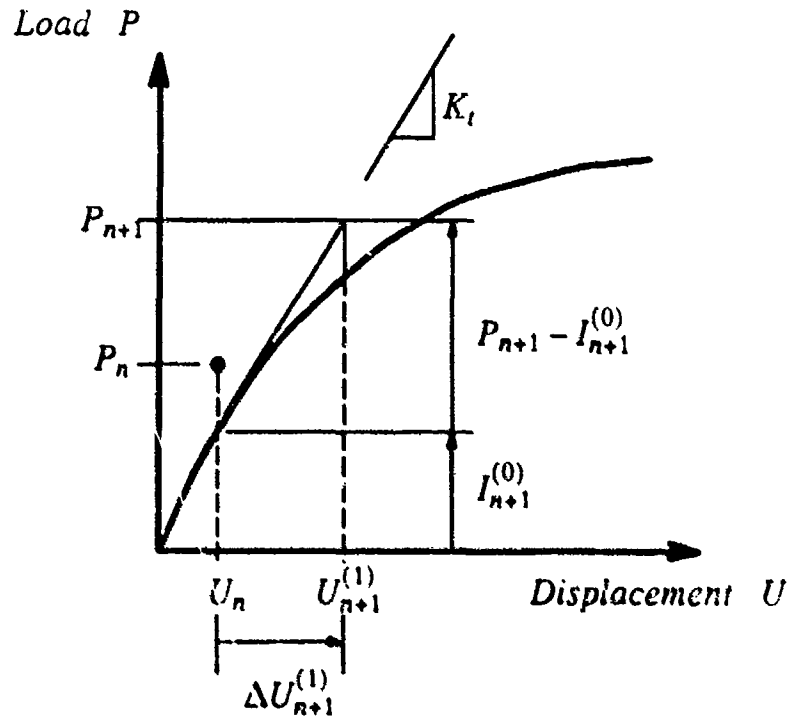


Fig. 4 Incremental - Iterative Solution of Nonlinear Structural Equilibrium Equations

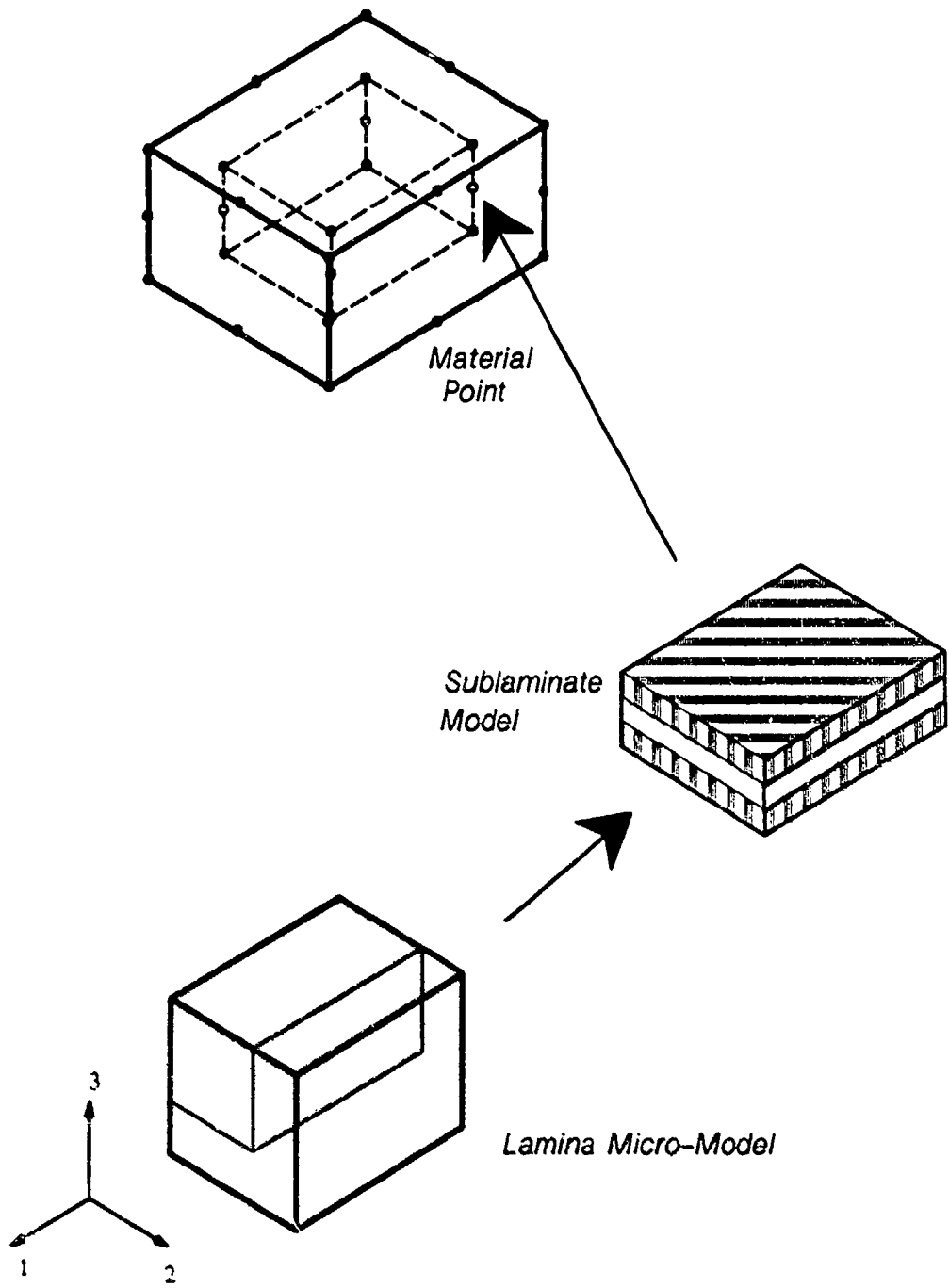
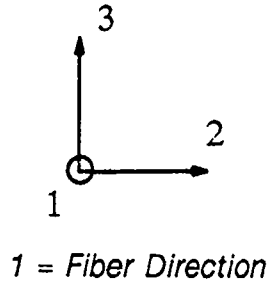
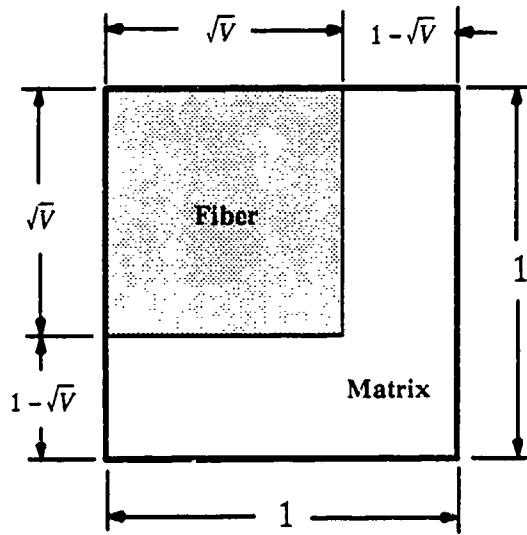
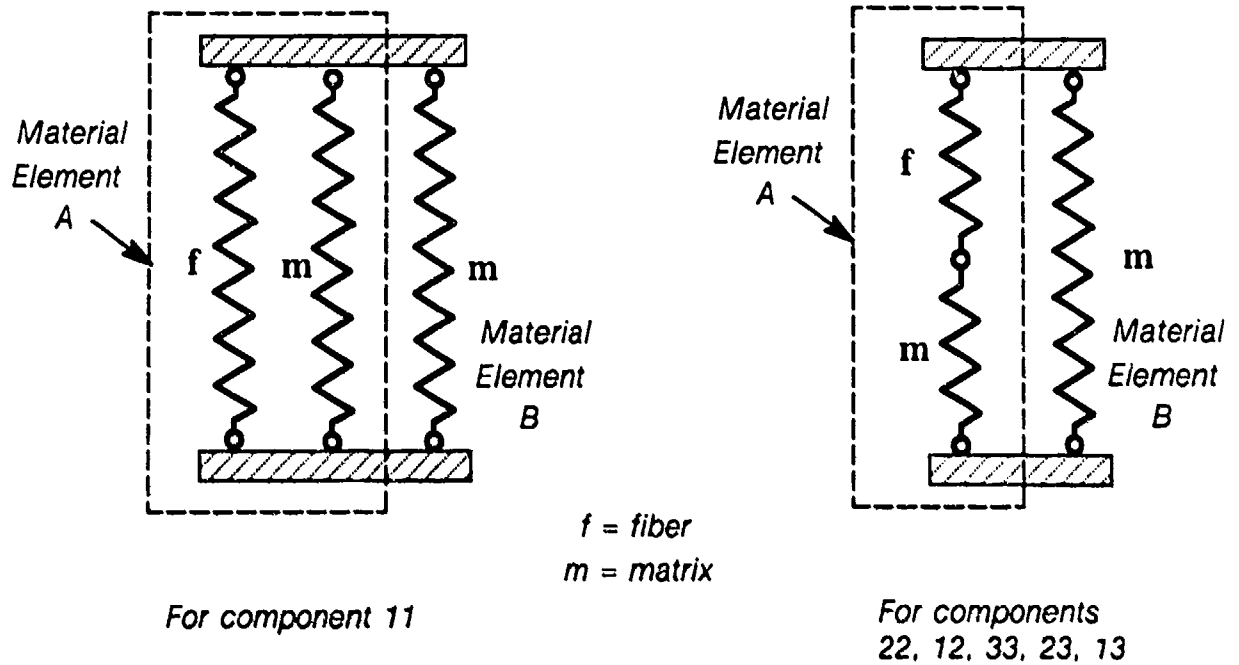


Fig. 5 Material Model for Thick-Section Modeling



Unit Cell ($V = \text{Fiber Volume Fraction}$)



Analogs for Stress and Strain Smearing in Unit Cell

Fig. 6 Micro-model for lamina

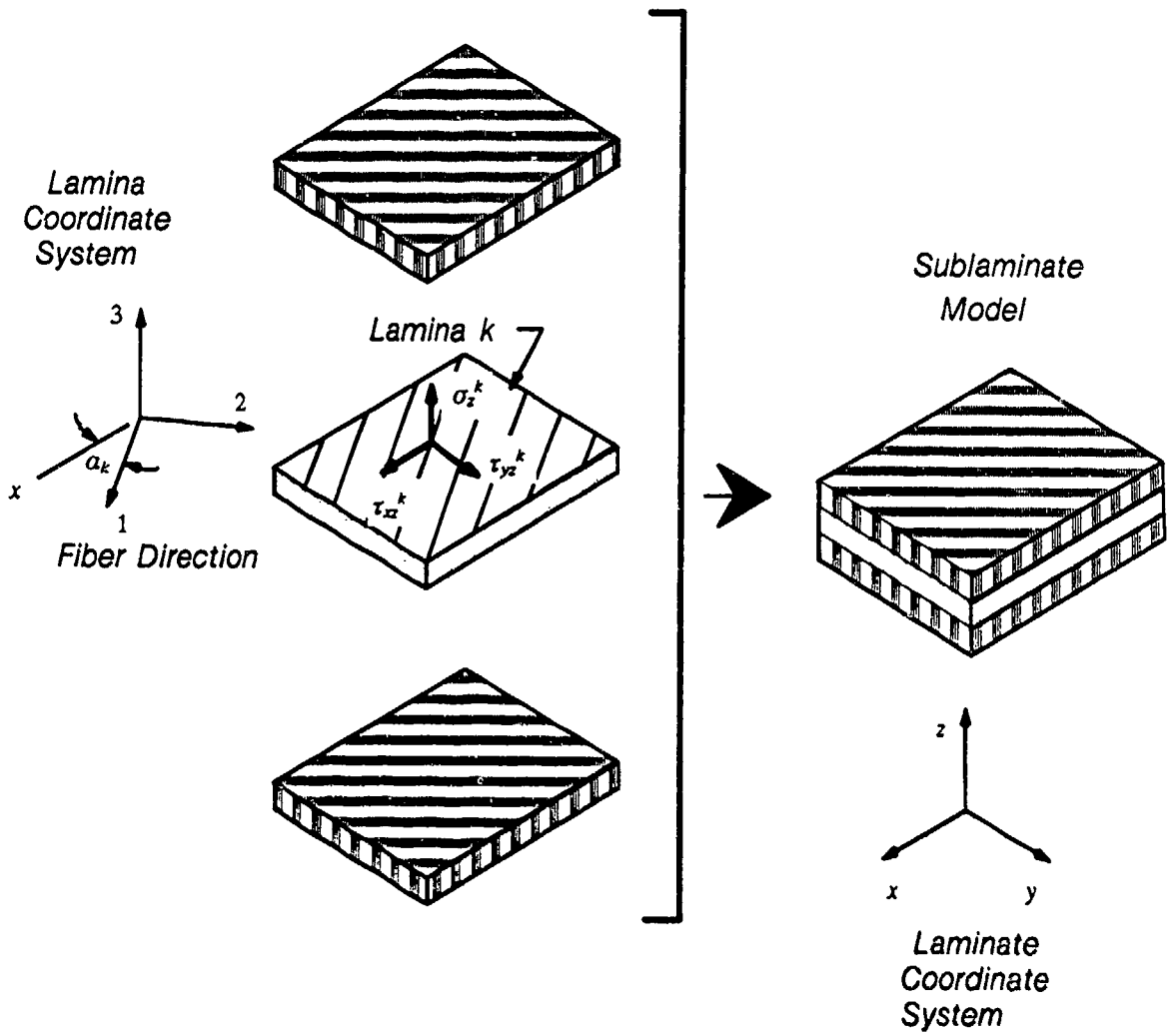


Fig. 7. Sublamine Model

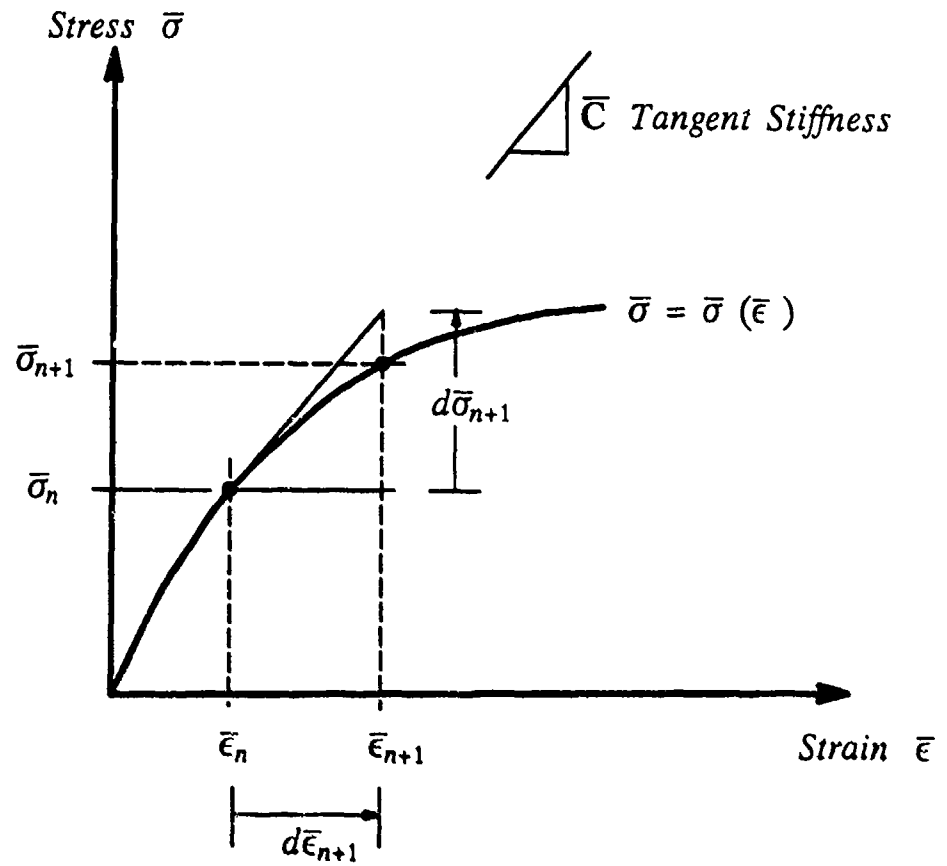


Fig. 8 Schematic (one-dimensional) View of Stress Update
 Illustrating the difference between $\bar{\sigma}_n$ and $\bar{\sigma}_n + d\bar{\sigma}_{n+1}$

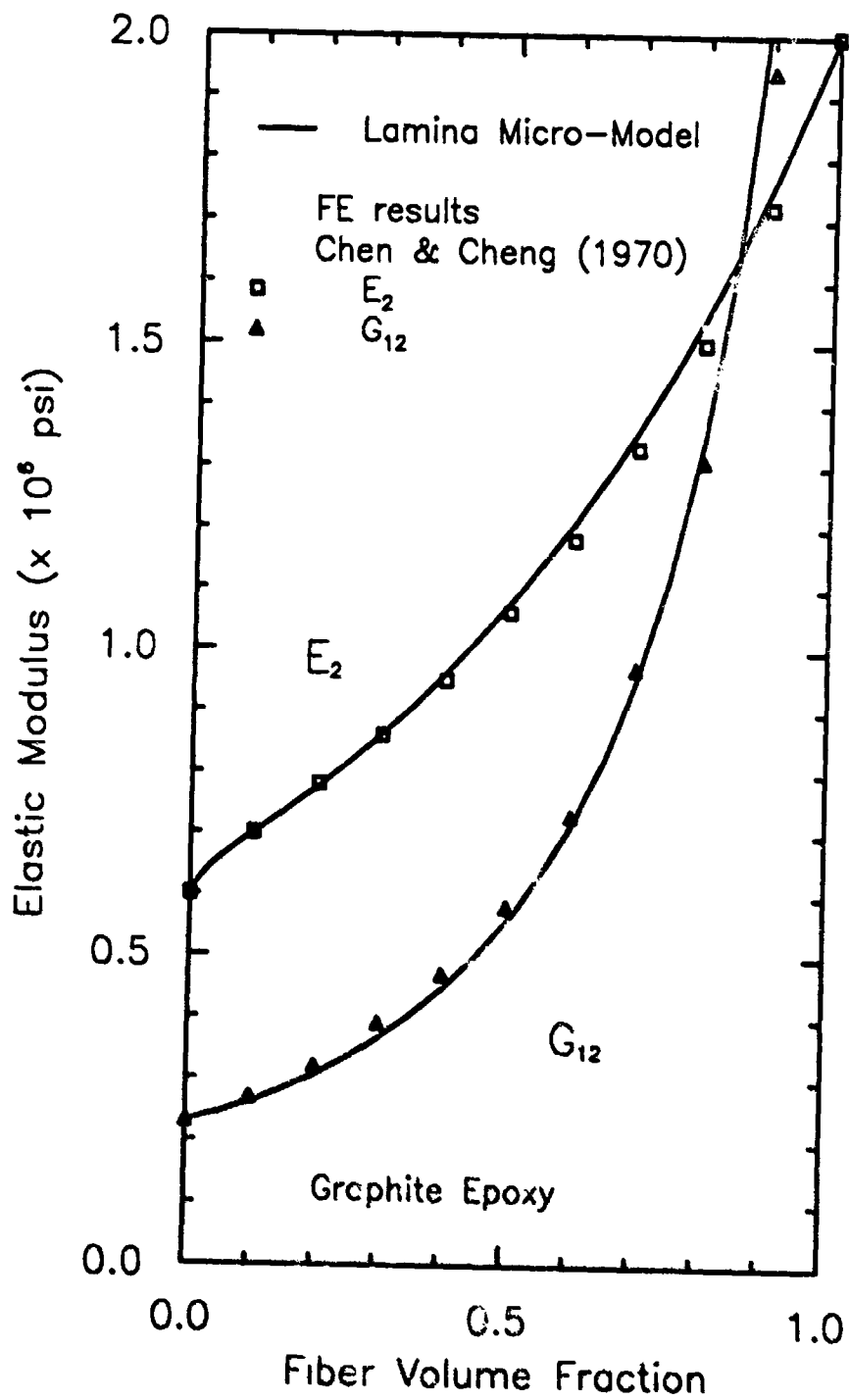


Fig. 9. Lamina Micro-Model vs FE micromechanical modeling

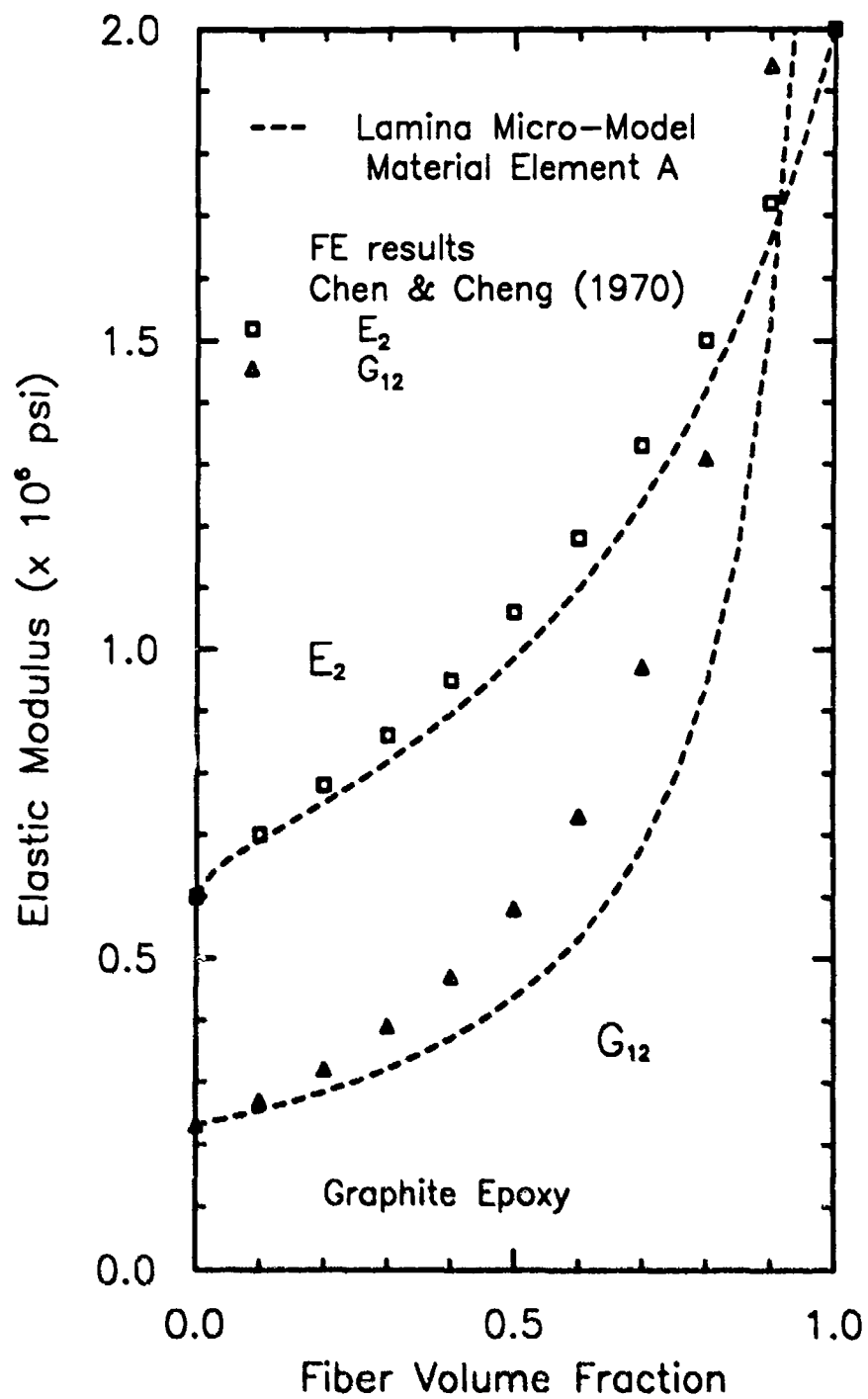
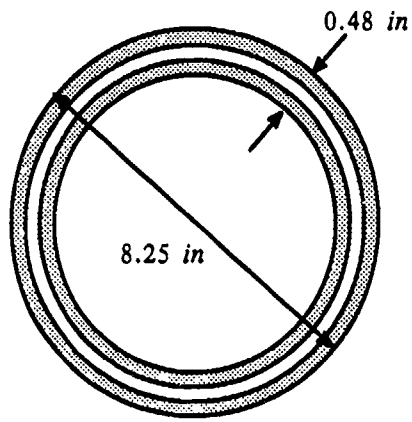
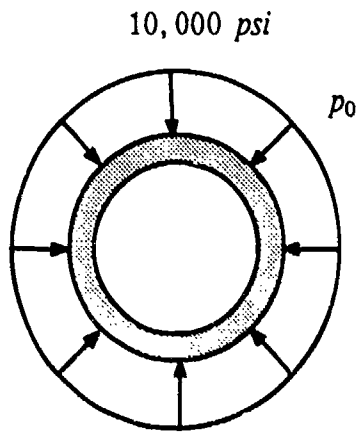


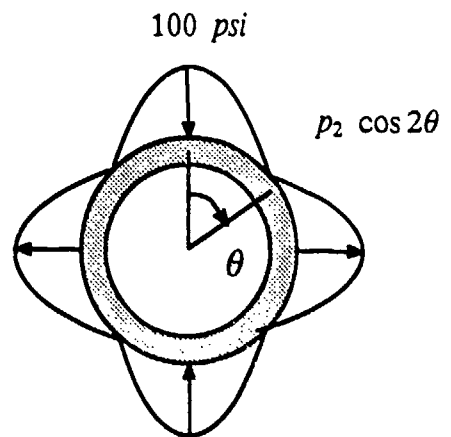
Fig. 10. Lamina Micro-Model - Material Element A only



Model Cylinder

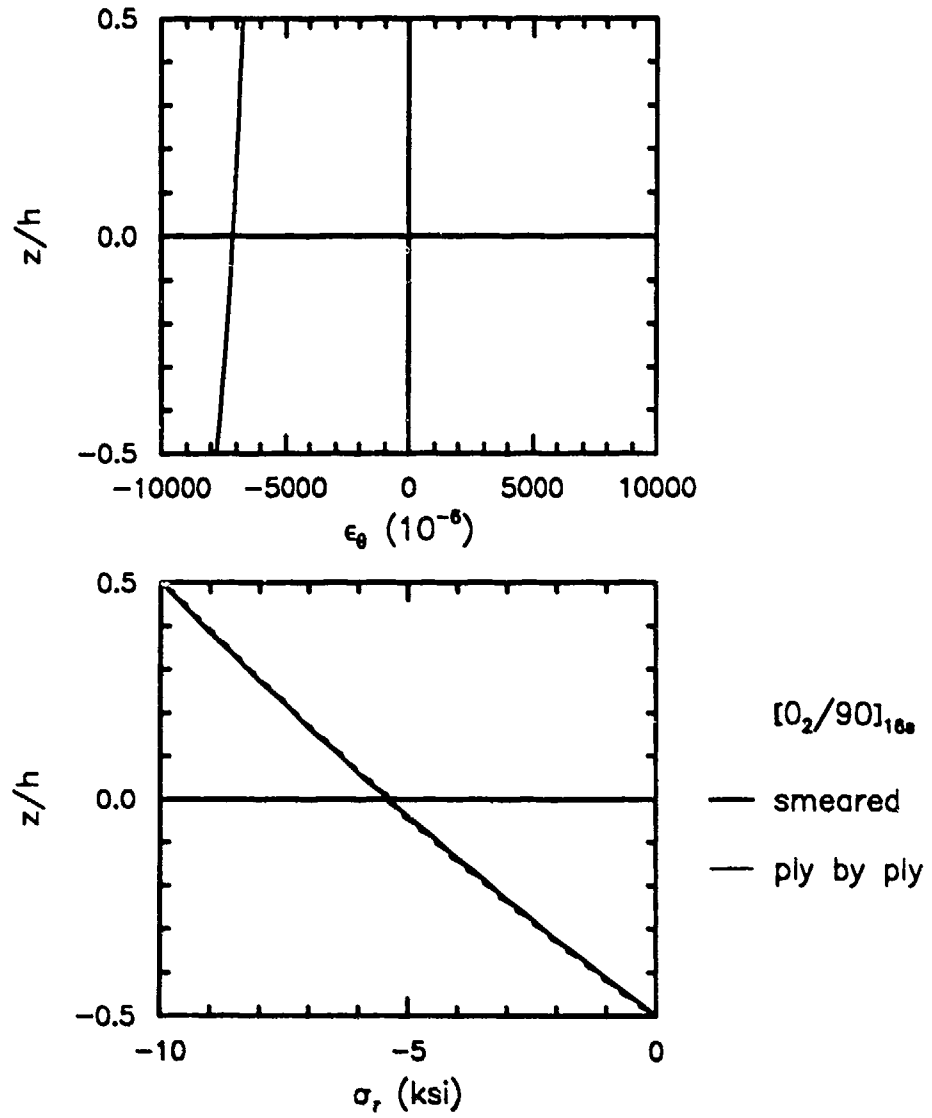


Compression



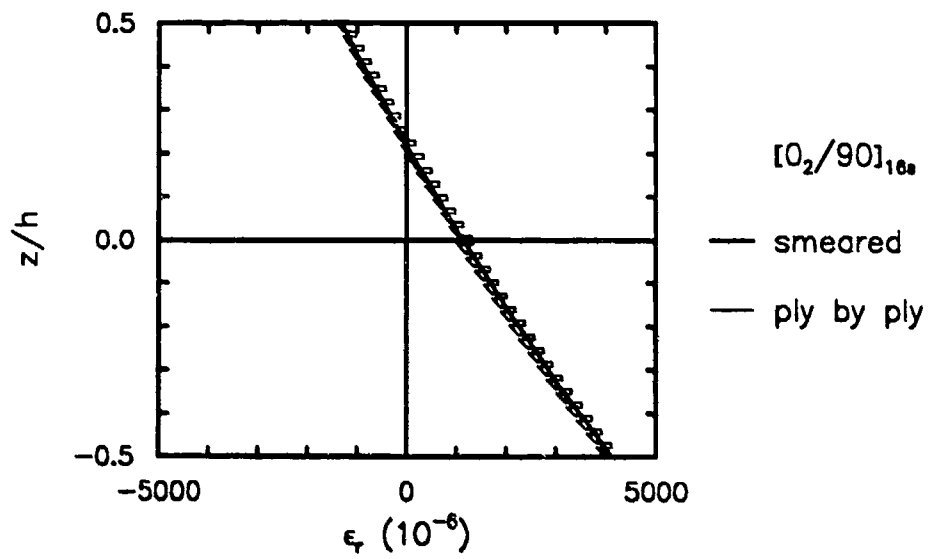
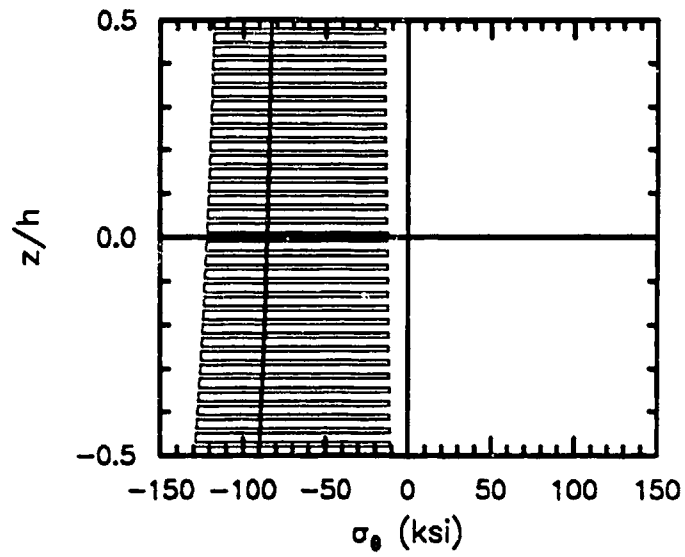
Bending

Fig. 11. Thick-Walled Model Cylinder



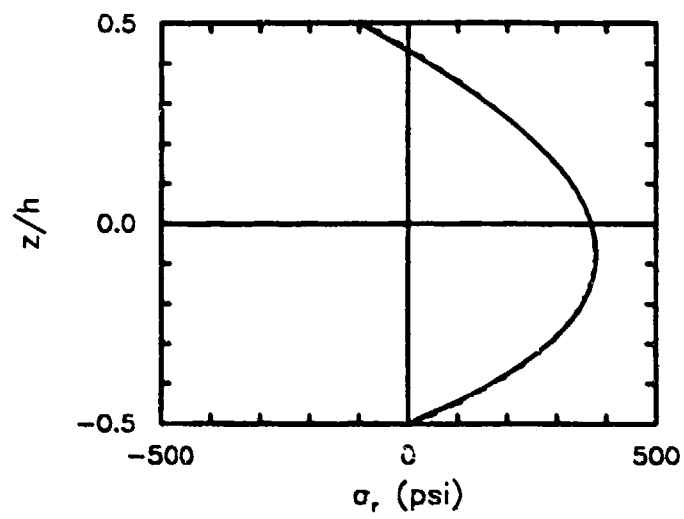
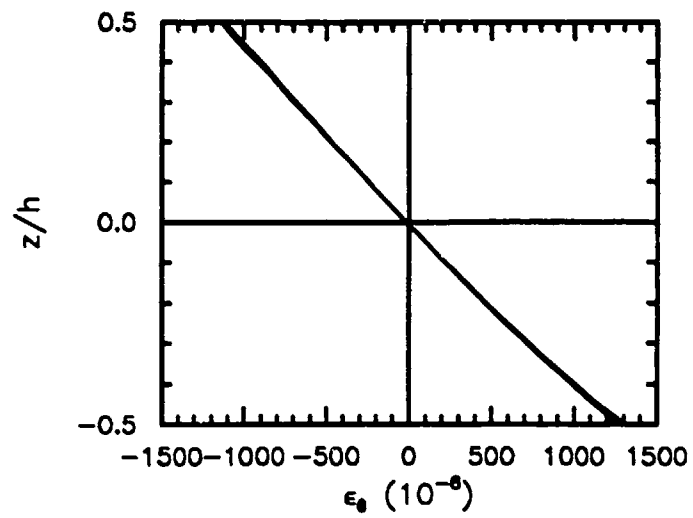
a. Continuous Responses ϵ_θ , σ_r , $\tau_{r\theta}$

Fig. 12. Compression Response of $[0_2 / 90]_{16s}$

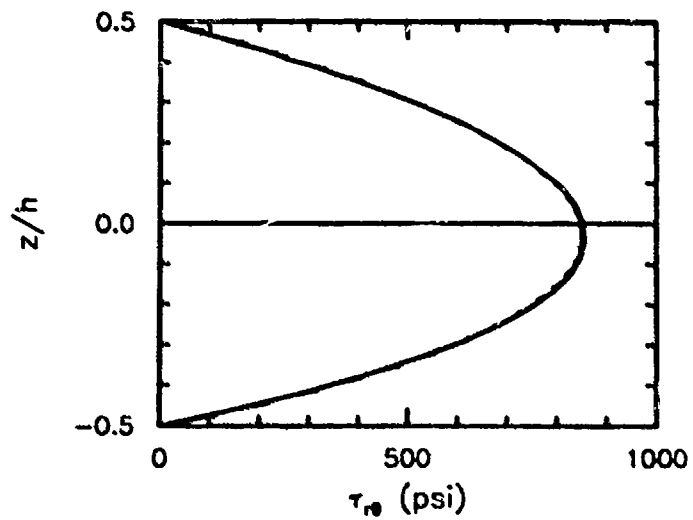


b. Discontinuous Responses σ_θ , ϵ_r , $\gamma_{r\theta}$

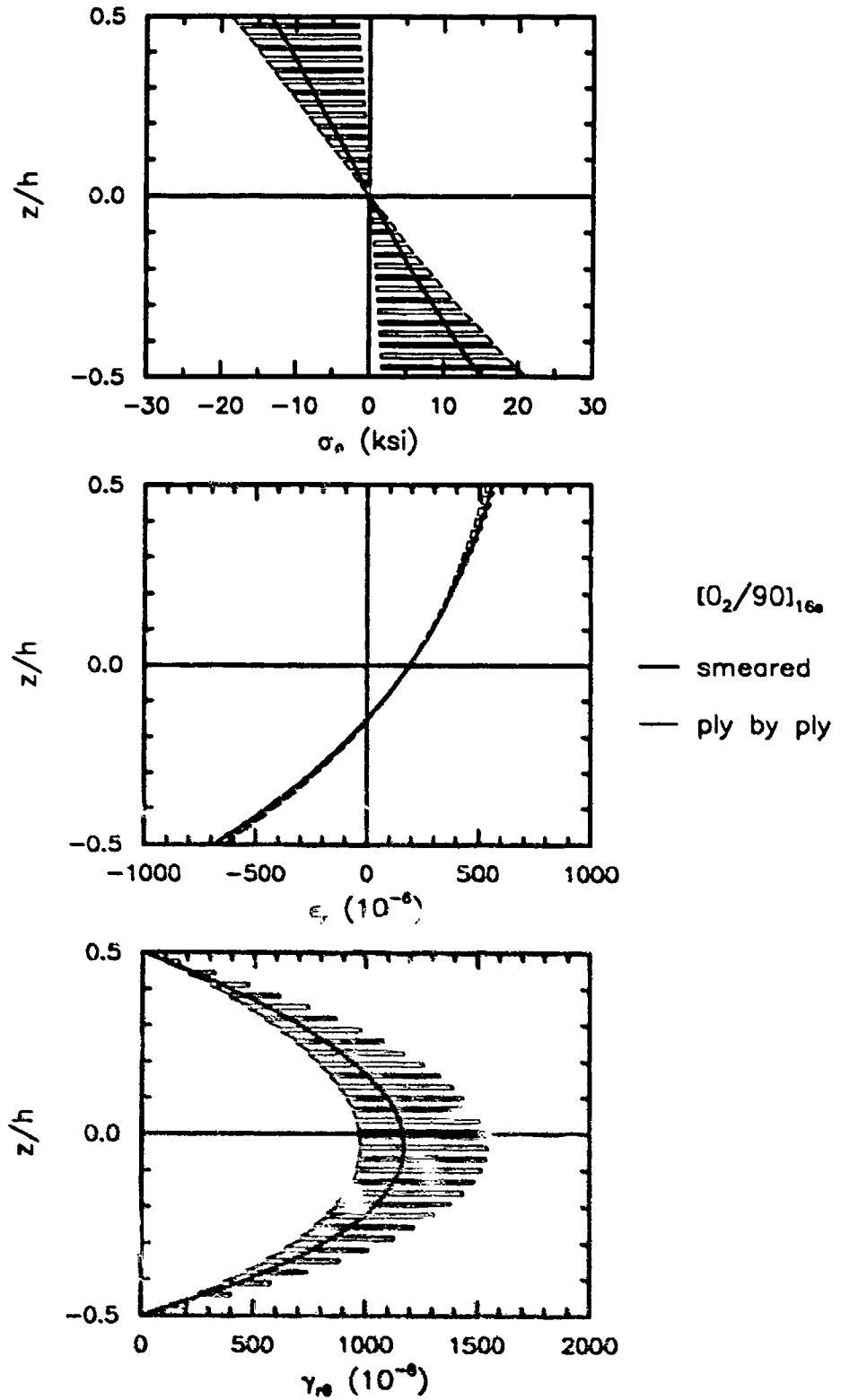
Fig. 12 Compression Response of $[0_2 / 90]_{16s}$



$[0_2/90]_{16s}$
 — smeared
 — ply by ply

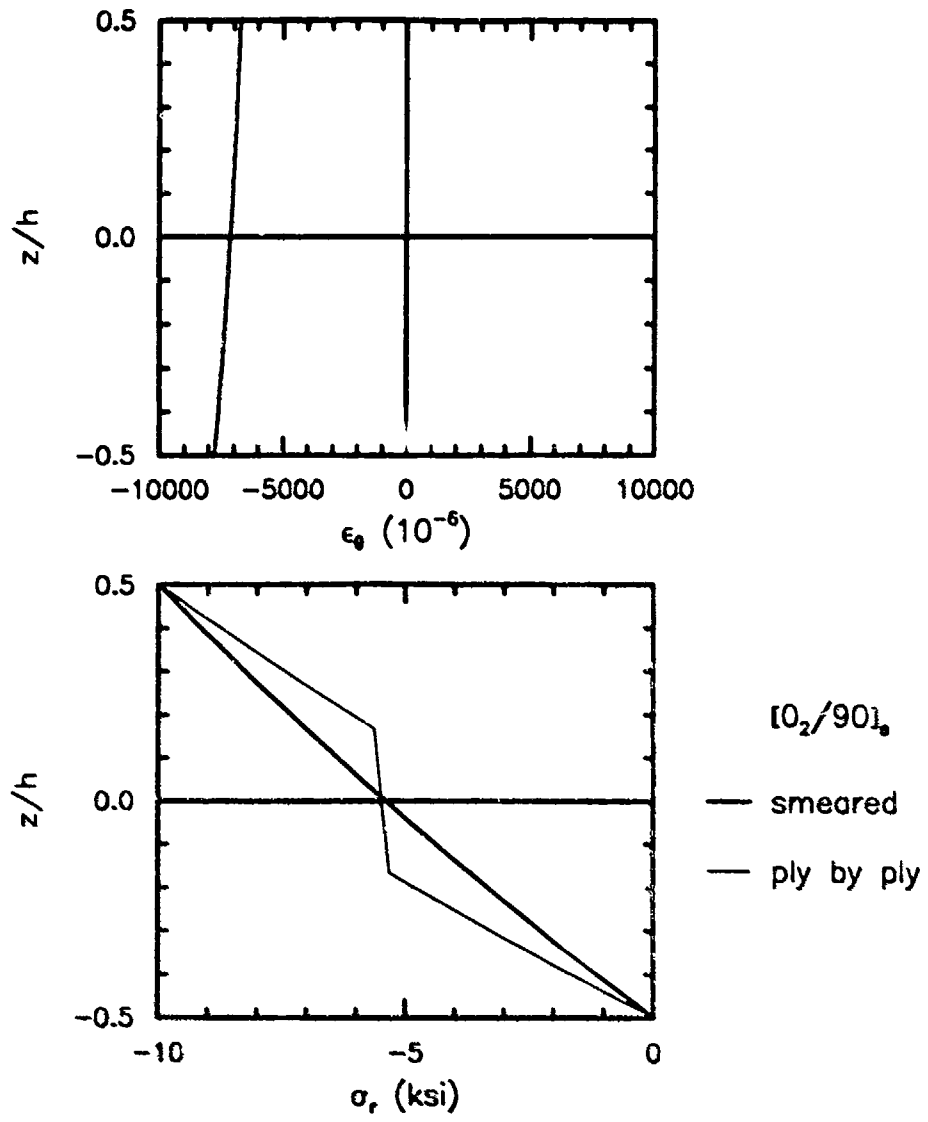


a. Continuous Responses ϵ_{θ} , σ_r , $\tau_{r\theta}$
 Fig. 13. Bending Response of $[0_2 / 90]_{16s}$



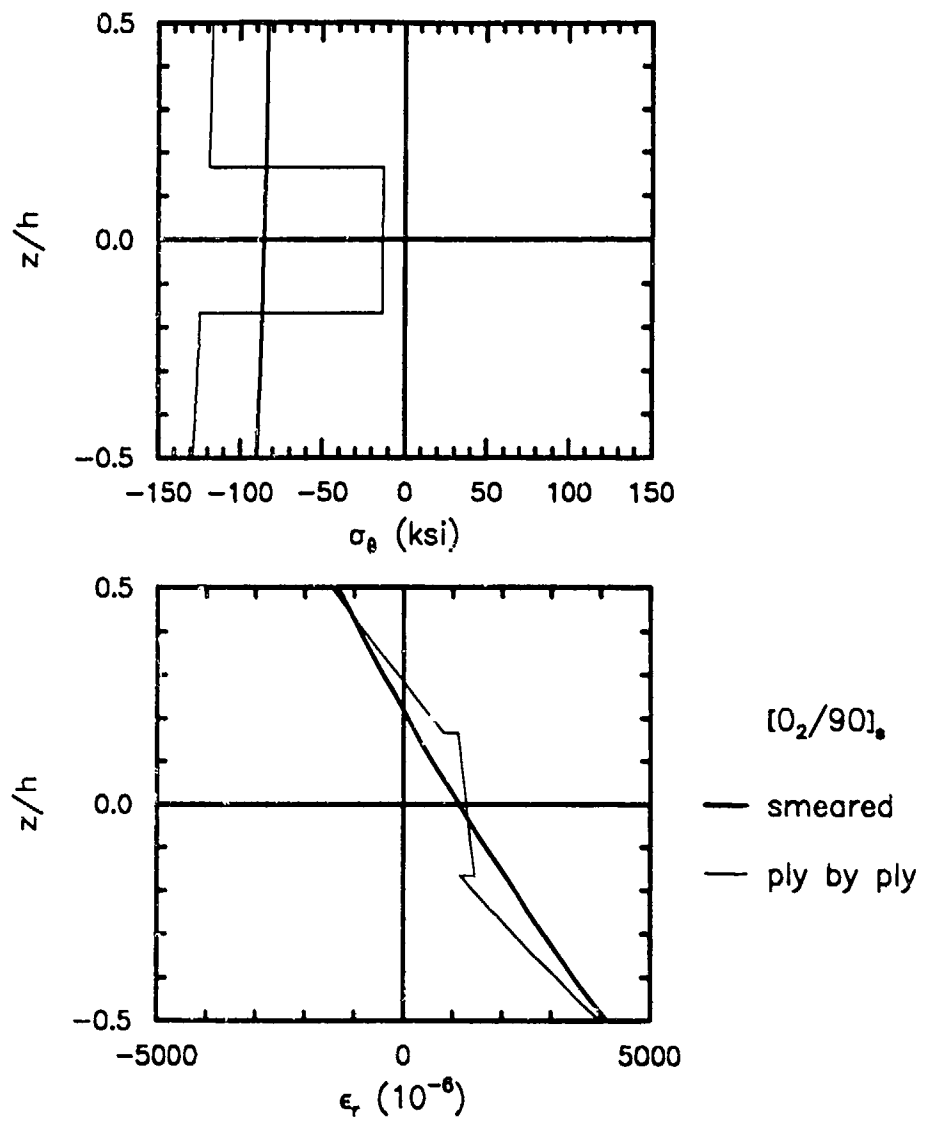
b. Discontinuous Responses σ_{θ} , ϵ_x , γ_{xz}

Fig 13. Bending Response of $[0_2 / 90]_{16s}$



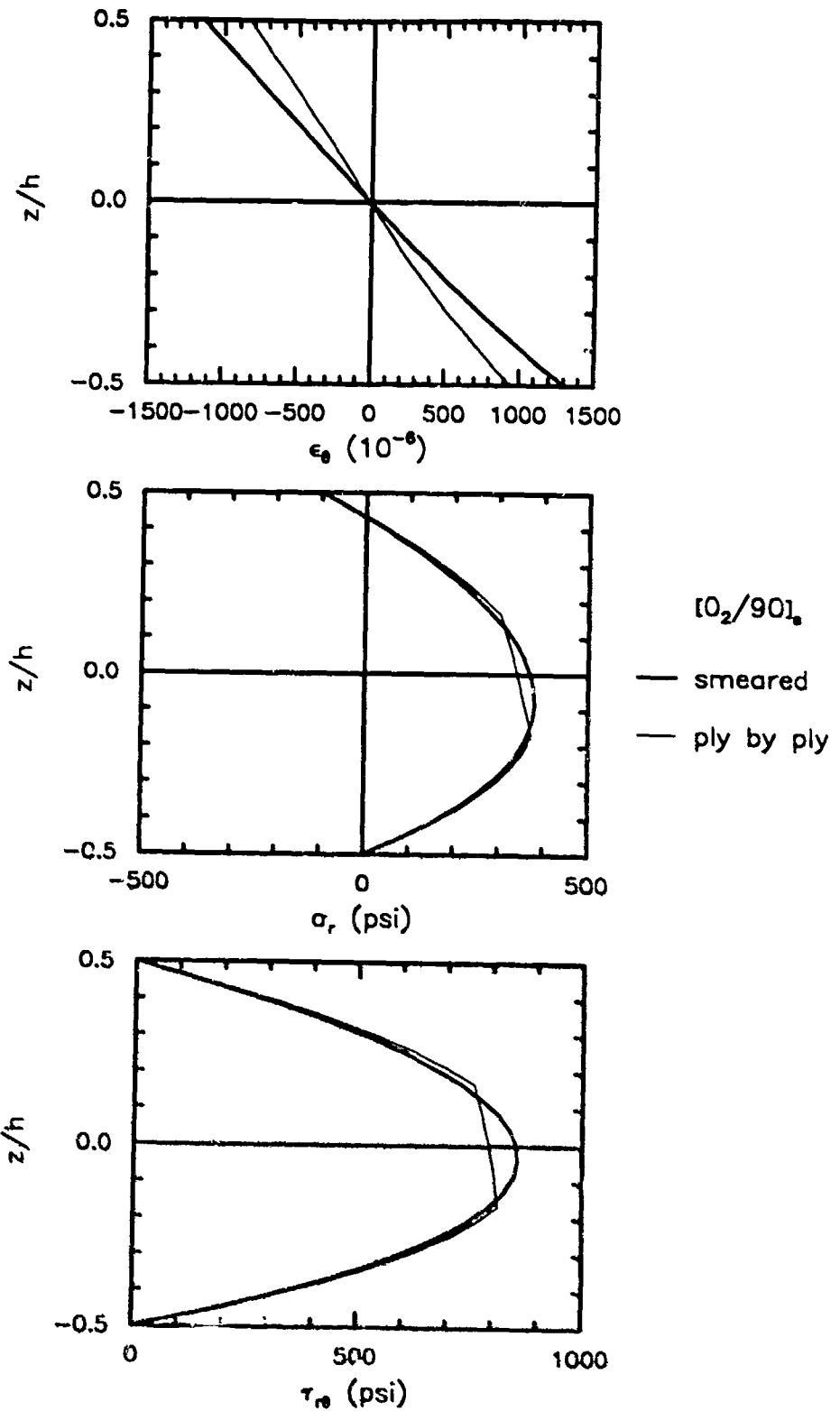
a. Continuous Responses ϵ_θ , σ_r , τ_{rz}

Fig. 14. Compression Response of $[0_2 / 90]_s$



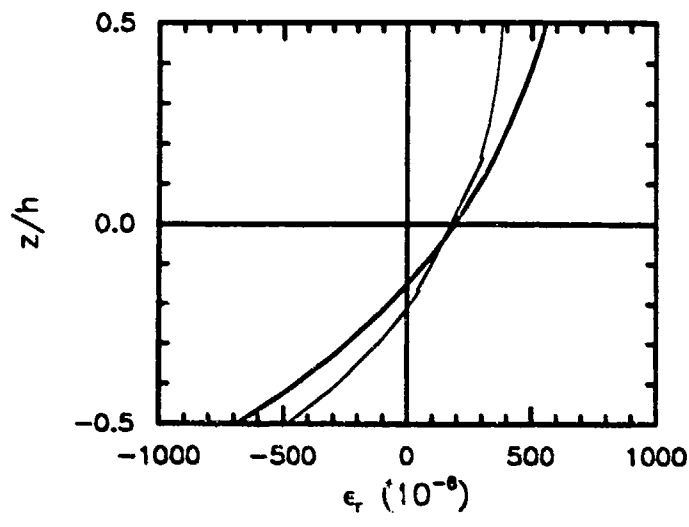
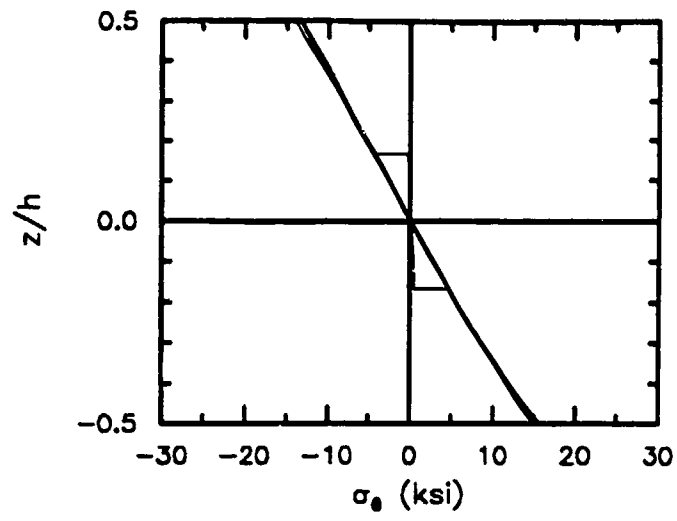
b. Discontinuous Responses σ_θ , ϵ_θ , $\gamma_{\theta z}$

Fig. 14. Compression Response of $[0_2 / 90]_s$

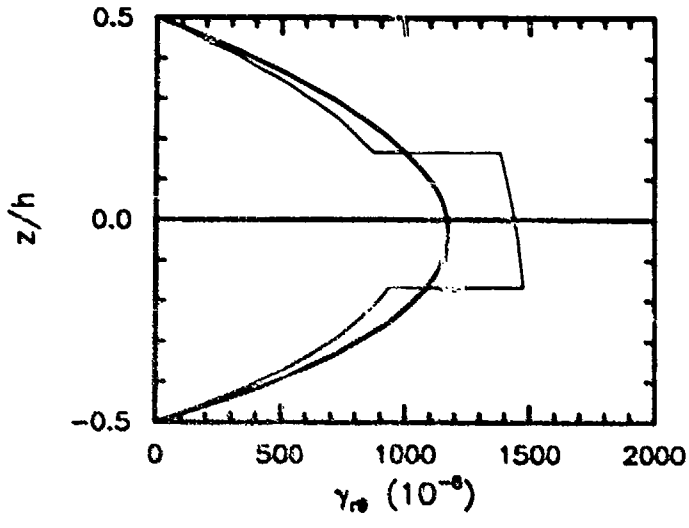


a. Continuous Responses ϵ_θ , σ_r , $\tau_{r\theta}$

Fig. 15. Bending Response of [0₂ / 90]_s



$[0_2/90]_s$
 — smeared
 — ply by ply



b. Discontinuous Responses σ_0 , ϵ_r , γ_{r0}

Fig. 15. Bending Response of $[0_2 / 90]_s$

INITIAL DISTRIBUTION

Copies		CENTER DISTRIBUTION
		Copies Code Name
5	ONR	
	1 Code 1132SM, Rajapakse	1 0115 Caplan
	1 Code 1131S, Dr. Fishman	1 0113 Douglas
	1 Code 1132SM, Barsoum	1 17 Krenzke
	1 Code 1216, Vasudevan	1 1702 Corrado
	1 Code 1132SM, Dr. Jones	1 172 Rockwell
2	ONT	1 176 Sykes
	1 Code 225, Kelly	5 1720.2 Phyllaier
	1 Code 233, Remmers	1 1720.4 Wiggs
3	NRL	1 1730.2 Critchfield
	1 Code 6380, Badaliance	1 2723 Wilhelmi
	1 Code 6383, Dr. Wolock	1 274 Wang
	1 Code 6385, Chaskelis	1 28 Wacker
5	NAVSEA	1 2801 Crisci
	1 Code 05M3, Pinto	10 2802 Morton
	1 Code 92R, Swann	25 2802 Camponeschi
	1 Code 92R, Spero	1 2803 Cavallaro
	1 Code 55Y2, Provencher	1 2814 Montiel
	1 Code 55Y2, Will	1 284 Fischer
1	NSWC, Code R31, Dr. Augl	1 2844 Castelli
		1 342.2 TIC Annapolis
12	DTIC	2 3431 Office Services

REPORT DOCUMENTATION PAGE

OMB No. 0704-0188

Public reporting burden for this collection of information is estimated to average 1 hour per response, including the time for reviewing instructions, searching existing data sources, gathering and maintaining the data needed, and completing and reviewing the collection of information. Send comments regarding this burden estimate or any other aspect of this collection of information, including suggestions for reducing this burden, to Washington Headquarters Services, Directorate for Information Operations and Reports, 1215 Jefferson Davis Highway, Suite 1204, Arlington, VA 22202-4302, and to the Office of Management and Budget, Paperwork Reduction Project (0704-0188), Washington, DC 20503.

1. AGENCY USE ONLY (Leave blank)	2. REPORT DATE October 1990	3. REPORT TYPE AND DATES COVERED	
4. TITLE AND SUBTITLE A Framework for 3-D Nonlinear Modeling of Thick-Section Composites		5. FUNDING NUMBERS	
6. AUTHOR(S) David A. Pecknold		8. PERFORMING ORGANIZATION REPORT NUMBER DTRC SME-90-92	
7. PERFORMING ORGANIZATION NAME(S) AND ADDRESS(ES) David Taylor Research Center Bethesda, MD 20084-5000		10. SPONSORING / MONITORING AGENCY REPORT NUMBER	
9. SPONSORING / MONITORING AGENCY NAME(S) AND ADDRESS(ES) David Taylor Research Center Bethesda, MD 20084-5000		11. SUPPLEMENTARY NOTES	
12a. DISTRIBUTION / AVAILABILITY STATEMENT Approved for Public Release. Distribution is unlimited.		12b. DISTRIBUTION CODE	
13. ABSTRACT (Maximum 200 words) <p>An architecture is proposed for three-dimensional nonlinear material modeling of thick-section composite laminates, which may have thicknesses ranging from 1/4 in. up to several inches. In this thickness range, there is very little applications-related experience or experimental information available; the potential effects of out-of-plane stresses and strains on material properties and behavior are therefore of great concern.</p> <p>The material model is intended to be used as a component of a standard finite element structural analysis package; this places severe practical limits on material model complexity. The model consists of two main components: a lamina micro-model containing fiber and matrix elements and a simplified unit-cell analysis; and a sublaminar model based on a 3D lamination theory which enforces equilibrium of out-of-plane stresses.</p>			
14. SUBJECT TERMS			15. NUMBER OF PAGES
17. SECURITY CLASSIFICATION OF REPORT Unclassified			16. PRICE CODE
18. SECURITY CLASSIFICATION OF THIS PAGE Unclassified	19. SECURITY CLASSIFICATION OF ABSTRACT Unclassified	20. LIMITATION OF ABSTRACT	